

## Quark and gluon distributions at the earliest stage of heavy-ion collisions

A. Makhlin

*Department of Physics and Astronomy, Wayne State University, Detroit, Michigan 48202*

(Received 27 December 1994)

Using the general framework of quantum field kinetics we consider new principles to compute initial distributions of quarks and gluons after the first hard interaction of heavy ions. We start by rewriting the integral equations of QCD in a form which is a generalization of the familiar QCD evolution equations. These equations describe both space-time and  $(x, Q^2)$  evolution before the collision and allow one to use the  $ep$  DIS data without reference to parton phenomenology. A new technique generates perturbation theory that avoids double counting of the processes, does not contain an artificial factorization scale, and does not require low-momentum cutoffs since infrared behavior is controlled by the DIS data.

PACS number(s): 25.75.+r, 12.38.Bx, 12.38.Mh, 24.85.+p

### I. INTRODUCTION

Recently, there have been many calculations [1–4] of the initial distributions of quarks and gluons in heavy-ion collisions, which may then lead to the creation of a plasma. In this paper, we do not consider the later stages of evolution which possibly lead to equilibration, or even the formation of a hydrodynamic regime. Instead, we shall concentrate only on the problem of the first quantum transition which converts two initial state composite systems—the stable nuclei in the “normal” nonperturbative vacuum—into a dense system of quarks and gluons which has a perturbative vacuum as its ground state.

Any strict formulation of a quantum-mechanical problem requires an exact definition of two main elements: the initial state of the system, and the observables in the expected final state.

(1) *The initial state.* Ideally, as in, for example, an atomic collision, we would define the initial state via its wave function. The wave functions of QCD nuclei are unknown. A natural alternative is to use the density matrix to describe each nucleus.

Here we may assume nuclei to be well shaped objects. The uncertainty of their boundaries does not exceed the typical Yukawa interaction range. In the laboratory frame, both nuclei are Lorentz contracted to a longitudinal size  $R_0/\gamma \sim 0.1$  fm. The tail of the Yukawa potential is contracted in the same proportion. The world lines of the nuclei are two opposite generatrices of the light cone that has its vertex at the interaction point. No interaction between nuclei is possible before they overlap geometrically. For this reason the total density matrix of two nuclei is a direct product of the two individual density matrices. The spaces of states where they act do not overlap either.

Since no exact information about the initial state of the nuclei is available, it seems reasonable to rely upon the following two considerations. First, detailed information is inessential as it basically relates to the interactions which maintain every nucleus as a QCD bound state. The energy of the collision is incomparably higher.

It is thus enough to require that the density matrix yields the given total momentum and the baryonic charge as averages of the corresponding field operators. Second, the residual dynamical information must reveal itself in the same way as in other inelastic processes at extreme energies, like deep inelastic electron-proton or muon-nucleus scattering (DIS). This statement may appear trivial, because structure functions of DIS are always used to account for this information. However, one should keep in mind that their definition—which does not refer to the parton model—is valid only for the DIS process itself. In order to apply structure functions to other interactions, using the parton model is considered unavoidable.

The first priority of this study is to avoid any intermediate phenomenology. We insist that any information taken from parallel experiments is valuable only as long as both processes can be described by the same theory and with the same initial data.

(2) *The final state.* The final state is assumed to be some distribution of free quarks and gluons in the perturbative vacuum. This vacuum is considered to be the true ground state, and is free of QCD condensates. It is a product of the nuclear collision and is postulated to exist in a sufficiently large volume. The spectrum of possible states of quarks and gluons after the collision is continuous. These states did not exist before the collision and are unoccupied at the beginning of the collision.

It is supposed also that the information which is most important for understanding the future evolution is concentrated in the single-particle distributions of quarks and gluons. These distributions must be calculated from their quantum-mechanical definitions, keeping in mind how they are to be measured in a hypothetical experiment. Two- and more-particle distributions should be defined as independent elements corresponding to other measurements.

In this work we rely heavily on a previous paper [5], where integral equations of QCD were derived without assuming that averaging is performed over a stationary state. To some extent these equations resemble the diagrammatic technique of Keldysh [6], which was designed

for nonequilibrium processes. They are of the same matrix form, but are not derived with a view to obtaining quasiclassical kinetic equations. Fields and their correlators remain the main objects of these equations and no phase-space distributions are introduced. For this reason the approach was named “quantum field kinetics” (QFK).

These new equations are the result of an initial resummation of the perturbation series for probabilities of inclusive processes (or any other observables). On the one hand, these new equations create an approach which proves to be very effective for studying various inclusive processes. On the other, they allow one to trace the temporal evolution of a colliding system, beginning from preparation in the past right up to the moment of measurement. This latter feature makes the new approach extremely attractive for our goals: The evolution of any physical system is completely defined by the initial data, and the act of measurement only selects one or more of all the possible quantum trajectories. Therefore one can expect that results of similar types of measurement will be similar. In this paper, we want to consider two similar processes, viz., deep inelastic electron-proton scattering and “deep inelastic  $pp$  or  $AA$  collisions,” in parallel.

To begin with, we must define the observables of these two processes in the same way. Definitions of inclusive amplitudes and inclusive probabilities to find one-quark or one-gluon excitations in the perturbative vacuum in the final state are given in Sec. II. The DIS cross section, viewed as an inclusive process where nothing is measured except the momentum of the scattered electron, is defined in the same terms at the beginning of Sec. III. The rest of this section considers an instructive example of the lowest-order calculations using a model density matrix. This calculation allows one to introduce all spinor and vector functions without extra complicated notation, and to clarify the complete calculation.

The dynamical equations in their full tensor-spinor form are derived in Sec. IV. It immediately becomes clear that these equations have a ladder structure. It appears that the well known ordering of ladder cells by Feynman  $x$  and virtuality is a direct consequence of the retarded temporal ordering inherent in these equations in their coordinate form. Smaller  $x$  and bigger virtualities correspond to the later times. Thus, as a by-product, we obtain an answer to a very old question about such correspondence [7–9].

The new equations appear to be richer than the usual QCD evolution equations for DIS structure functions, as derived from the renormalization group approach. The new evolution equations interconnect two invariant functions of the vector field, and two of the quark field. These equations do not depend upon the type of latest interaction; however, they may be projected onto any definite process. Specific properties of the “last” electromagnetic interaction select only one of the spinor functions into the definition of the structure function  $F_2$  of unpolarized DIS. However, both quark field functions remain in the evolution equations, along with the two functions of the vector field. The relative scale of additional terms and their possible role are examined in Appendix A.

The meaning of the objects that obey the new evolution equations comes to light in a discussion of renormalization. The renormalization group approach cannot be used here, if only because most of the terms in these equations correspond to observables (imaginary parts of self-energies), are finite, and may not be renormalized. Instead, we renormalize the second subgroup of the evolution equations for the real part of the self-energies using a conventional Bogolyubov-Hepp-Parasyuk-Zimmerman (BHPZ) scheme. Ultraviolet divergencies are compensated for by counterterms from the original Lagrangian. The running coupling appears precisely from the requirement of renormalizability. For the moment, this part of the study is at the level of a basic idea.

Using some structural, rather than quantitative, assumptions and after projecting onto specific observables of the  $e$ - $p$  DIS, the new equations can be reduced to the system of the Gribov-Lipatov-Altarelli-Parisi (GLAP) equations [10–12]. The objects which enter the new equations are similar to self-energies, and we shall call them sources. It appears that the QCD evolution proceeds in such a way as to create a source of a field which interacts with the detector in a certain way. The evolution causes the dynamical assembly of a special wave packet which represents a quark or gluon which is “properly prepared for the last interaction.” This process takes place in real time and ends at the moment of interaction.

In Appendix A it is also shown that the new equations naturally reduce to the Balitskij-Fadin-Kuraev-Lipatov (BFKL) [13] equation, and that they are capable of describing the effects of quark and gluon shadowing at small  $x$ . The resulting shadowing terms appear to be parametrically larger than those in previous derivations [14,15].

We expect DIS to provide the dynamical information about this process. This information is valuable only as long as no measurements were done before the last interaction. All unobserved information (and providing it was not observed) is included in the definition of the sources with their full dependence upon  $x$  and  $Q^2$ .

Here, we do not adhere to the picture of “wee partons,” and do not share the opinion that the QCD evolution equations describe how one valence quark develops a cloud of virtual quarks and gluons around it at small distances. We believe that they give (perturbatively) the “evolution” of the detector response, provided the trigger includes the requirement of a bare on-shell quark in the final state (which usually may be expressed as the resonant condition  $x_{Bj} = x_F$ ). That they definitely do not correspond to the evolution of a single quark is seen, for example, from the possibility of including fusion (shadowing) into the evolution equations.

The difference between the structure functions and the sources can be explained using an analogy: in condensed matter or scattering theory we introduce two different quantities, the density of states  $\rho(E)$  and the number of states below energy  $E$ ,  $n(E) = \int^E \rho(E)dE$ . The structure functions then correspond to  $n(E)$ , while the sources correspond to  $\rho(E)$ . In an experiment we measure  $n(E)$  (which is proportional to the allowed volume in the phase space), rather than  $\rho(E)$ . From this point of view it is not surprising that we eventually express observables,

roughly speaking, via the derivatives of structure functions like  $dG(x, Q^2)/dQ^2$ . Different measurements study these quantities, integrating them with their specific “upper limits.” The boundary conditions for  $x$  and  $Q^2$  evolution are imposed by the measurement, rather than the initial conditions which are controlled by momentum conservation, sum rules, etc. These must be set in the past without any relation to the  $(x, Q)$  evolution.

Cross sections of inclusive single-quark and single-gluon production in the lowest nonvanishing order are calculated in Sec. V. All of them contain scale-dependent and -independent terms. The latter are much bigger than the former, and as a result the cross sections are expected to exhibit only weak scale dependence. The lowest-order cross sections are strongly peaked at low rapidities and low transverse momenta.

The next order of the perturbative expansion generated by the new evolution equations is examined in Sec. VI. The new expansion does not lead to any diagrams which duplicate those already included in the definition of the sources (or structure functions). Any such diagrams would carry severe collinear singularities. We carefully examine the infrared finiteness of the diagrams that do occur. It is shown that they are infrared safe and that no artificial cutoffs are necessary to find the total cross section. Higher-order perturbation terms are not expected to present any difficulty, as their final state infrared behavior will be shielded by the final distributions themselves.

We are led to the approach advocated in this paper in an unavoidable manner. Ideally, one would start with a complete relativistic quantum description of the static proton and its interaction with the detector. Unfortunately, the many attempts to describe the bound states of QCD (see Refs. [16] and [17] for reviews) have not yet met with real success. To calculate the production of particles in hadronic collisions, one is limited to reasoning along the following lines: first, an operator product expansion (OPE) analysis of the DIS data, which gives the structure functions of DIS; next, a partonic interpretation of the structure functions; and, lastly, using the factorization technique. In the end, one still faces severe theoretical problems caused by the soft processes, the arbitrariness of the factorization scale, etc. Here, we try to avoid these problems “experimentally,” by maximizing the use of dynamic information hidden in the DIS data.

## II. SINGLE-PARTICLE DISTRIBUTIONS OF THE PARTONS

The entire scenario of the heavy-ion collision is very complicated. It is common to divide it into several stages dominated by different physical processes. Currently, each stage is described using a different approach. Quantum field kinetics (QFK) [5] was conceived as a formalism that allows one to describe all stages of the collision, including the transient ones, using the same technical tools. The theory should explicitly follow the temporal sequence of the stages, and allow for smooth transitions between them. In this paper we study the first hard pro-

cess which destroys coherence of the initial wave functions of the incoming hadrons (or nuclei). However, it is expedient to include a brief discussion of how the neighboring transient regions look and how the language of QFK may work there.

Before the collision, two nuclei  $A$  and  $B$ , with momenta  $P_A$  and  $P_B$ , move towards each other at almost the speed of light, and the center-of-mass system coincides with the laboratory frame. We assume that the center-of-mass energy is very large,  $s \gg M^2$ , so that the laboratory frame is the infinite momentum frame for both nuclei. The “infinite momentum frame” is a synonym of the “light-front dynamic,” a very complicated object, which had been introduced by Dirac [18] long ago, along with the other forms of the dynamic. According to Dirac, every (Hamiltonian) dynamic includes its specific definition of the quantum-mechanical observables on the (arbitrary) spacelike surfaces, as well as the means to describe evolution of the observables from the “earlier” spacelike surface to the “later” one. Besides the light-front dynamics, Dirac has also suggested the so-called point form of field dynamics which was conceived as a tool to describe the interaction of the field with the pointlike classical particle.

The applicability of the light-front form of dynamic to the DIS process, the proton interaction with the structureless electron, is indisputable. However, in the more complicated case of the two-hadron (or two-nucleus) collision, both composite objects should be described using the same dynamic. This requirement follows solely from the fact that the definition of the field states (particles) depends on how the observables are defined. This is most important for gluons: the choice of the gauge is one of the elements of the Hamiltonian dynamic. A suitable form of dynamic should be consistent with the Lorentz contraction of the nuclei. The idea of the collision of two plane sheets immediately leads us to the “wedge form:” All possible states of quark and gluon fields before and after collision should be confined to within the past and the future light cones (wedges) with the  $(x, y)$  collision plane as the edge.

It turns out to be possible to treat two different light-front dynamics as two limits of a single dynamic where the states of the quark and gluon fields are defined on the spacelike hypersurfaces of the constant proper time  $\tau$ ,  $\tau^2 = t^2 - z^2$ . Considering the collision as a kind of detector which performs a spectral analysis of the colliding composite systems, we restrict ourselves in advance to a class of states which can resonantly participate in the localized interaction. In this *ad hoc* approach, all the spectral components of the nuclear wave functions unavoidably collapse in the two-dimensional plane of interaction, even if all the confining interactions of quark and gluons in the hadrons are switched off, and if the coherence of the hadronic wave functions is destroyed.

A complete study of the wedge form of dynamic is underway now. The well known DIS structure functions remain as well defined elements of the joint dynamic. In what follows, we refer to the process of their formation (spectral decomposition of the nuclei into the proper set of modes) as the precollision dynamic. We rederive the

QCD evolution equations for the DIS structure functions and generalize them for the needs of our problem in the next two sections using the QFK language. As a result, we find how to extract maximum information from the DIS data and provide a smooth transition to the description of the later stages.

A qualitative understanding of the expected final state can be obtained by a “quantum kinematic” analysis of the extreme case when no dynamical information is required. Let the nuclei collide at an energy of about 100 TeV per nucleon, when the nuclear longitudinal size is only  $10^{-4}$  fm. This size is much less than any known in nuclear interactions, and one may consider the domain where the nuclei overlap as a plane surface [or a point in the  $(t, z)$  plane]. All the subsequent dynamics takes place within the future light cone of this point,  $t^2 - z^2 > 0$ ,  $t > 0$ . As the translation invariance in  $t$  and  $z$  directions is manifestly broken by the initial conditions, one should look for the appropriate quantum numbers (other than  $p^0$  and  $p^z$ ) to describe the final states of the particles. The symmetry that does survive is Lorentz invariance, and the relevant quantum number is the boost.

However, rather than the boost, it is more common to use the momentum as a quantum number of the particle. While in the geometry of a localized interaction there is no quantum operator for conserved momentum, we may find wave packets which behave as free plane waves, at least asymptotically. The wave packets with the required behavior are

$$\begin{aligned} \Xi_{y,p_\perp}(x) &= \frac{1}{4\pi^{3/2}} e^{-im_\perp \tau \cosh(\eta-y)} e^{i\vec{p}_\perp \vec{r}_\perp} \\ &= \frac{1}{4\pi^{3/2}} e^{-ip^0 t + ip^z z} e^{i\vec{p}_\perp \vec{r}_\perp}. \end{aligned} \quad (2.1)$$

These wave packets represent plane waves confined to within the future light cone of the collision point, and are normalized on the spacelike hypersurfaces  $\tau = \text{const}$ :

$$\begin{aligned} (\Xi_{y,p_\perp}^*, \Xi_{y',p'_\perp}) &= \int \tau d\eta d^2\vec{r} \Xi_{\nu,p_\perp}^*(x) i \overleftrightarrow{\frac{\partial}{\partial \tau}} \Xi_{y',p'_\perp}(x) \\ &= \delta(y - y') \delta(\vec{p}_\perp - \vec{p}'_\perp). \end{aligned} \quad (2.2)$$

Here, we use coordinates  $(t = \tau \cosh \eta, z = \tau \sinh \eta, \vec{r}_\perp)$ , and denote  $m_\perp^2 = m^2 + p_\perp^2$ ,  $p^0 = m_\perp \cosh y$ , and  $p^z = m_\perp \sinh y$ .

At large  $m_\perp \tau$ , the phase of the wave function  $\Xi_{y,p_\perp}$  is stationary in a very narrow interval around  $\eta = y$  (outside this interval, the function reveals oscillations with exponentially increasing frequency): the wave function describes a particle with rapidity  $y$ . However, for  $m_\perp \tau \ll 1$ , the phase of the wave function is almost constant along the surface  $\tau = \text{const}$ . The smaller  $\tau$ , the more uniformly the particle is spread along the light cone. Up to distortions caused by the finite size of the interaction domain, any high-energy collision will produce a distribution which is uniform in rapidity in the vicinity of the light cone. The picture looks as if the incoming nuclei carry this distribution *ab initio*. The latter is not surprising as the same arguments can be applied to the states of particles before a strongly localized interaction. The distribution  $dN \sim \text{const} \times dy$  corresponds to

$dN \sim \text{const} \times dx_F/x_F$  in terms of the Feynman variable  $x_F$ . Thus we arrive at a result which is typical for the Williams-Weiszacker approach. The full consideration for the QCD nucleus has been recently given by McLerran and Venugopalan [4]. We assume that deviation from this ideal distribution can be studied perturbatively with increasing accuracy the higher the energy of the collision is.

The realistic structure functions invoke the scale which is absent in the limit of infinite energy. They allow one to compute various distributions of quarks and gluons created after the first interaction of two nuclei. As we expect creation of a dense system, we consider the one-particle distributions to be most important. The inclusive amplitudes leading to the creation of one quark or one gluon from the initial state  $|\text{in}\rangle$  are as follows:

$$\langle X | d(\mathbf{p}, \sigma, i) S | \text{in} \rangle \quad \text{and} \quad \langle X | c(\mathbf{k}, \lambda, a) S | \text{in} \rangle, \quad (2.3)$$

where  $d^\dagger(\mathbf{p}, \sigma, i)$  is a creation operator for an on-mass-shell quark with momentum  $p$ , spin  $\sigma$ , and color  $i$ . Similarly, the operator  $c^\dagger(\mathbf{k}, \lambda, a)$  creates an on-mass-shell gluon with momentum  $k$ , polarization  $\lambda$ , and color  $a$ . Summing the squared moduli of these amplitudes over a complete set of uncontrolled states  $|X\rangle$ , and averaging over the initial ensemble, we find inclusive spectra of quarks and gluons

$$\frac{dN_q}{d\mathbf{p}} = \sum_{\sigma,i} S p \rho_{\text{in}} S^\dagger d^\dagger(\mathbf{p}, \sigma, i) d(\mathbf{p}, \sigma, i) S, \quad (2.4)$$

$$\frac{dN_g}{d\mathbf{k}} = \sum_{\lambda,a} S p \rho_{\text{in}} S^\dagger c^\dagger(\mathbf{k}, \lambda, a) c(\mathbf{k}, \lambda, a) S. \quad (2.5)$$

The initial state of the colliding system consists of two Lorentz-contracted nuclei which are causally independent, and thus the total density matrix is a direct product of two independent density matrices,

$$\rho_{\text{in}} = \rho_A \otimes \rho_B \otimes |0_{\text{cont}}\rangle \langle 0_{\text{cont}}|. \quad (2.6)$$

Matrix elements of  $\rho_{\text{in}}$  are obtained by sandwiching it between all state vectors  $|\text{in}\rangle$  which enter definition (2.3) of inclusive amplitudes. The density matrices  $\rho_A$  and  $\rho_B$  contain only bound states of quarks and gluons in the presence of vacuum condensates. The latter are assumed to be destroyed in the course of the initial hard collision and replaced by the perturbative QCD vacuum. Initially, all states in the continuum are unoccupied. This means that  $\rho_{\text{in}}$  contains a projector  $|0_{\text{cont}}\rangle \langle 0_{\text{cont}}|$  onto the vacuum state in the continuum. So we may commute the quark Fock operators with  $S$  and  $S^\dagger$  and only commutators survive in the final result:

$$\frac{dN_q}{d\mathbf{p}} = \sum_{\sigma,i} \int d^4x d^4y \bar{\psi}_{p,\sigma,i}^{(+)}(x) \left\langle \frac{\delta S^\dagger}{\delta \bar{q}_i(y)} \frac{\delta S}{\delta q_i(x)} \right\rangle \psi_{p,\sigma,i}^{(+)}(y). \quad (2.7)$$

In this expression  $\psi_{p,\sigma,i}^{(+)}(x)$  is the Dirac wave function of a quark. Summing over spin and color we get

$$\frac{dN_q}{d\mathbf{p}} = \sum_{\sigma,i} \int d^4x d^4y \frac{e^{-ip(x-y)}}{(2\pi)^3 2p^0} \text{Tr}[\not{p} i \Sigma_{01}^{ii}(x, y)], \quad (2.8)$$

where the full  $2 \times 2$  matrix of the quark self-energy is given by [5]

$$\begin{aligned} \Sigma_{AB}(x, y) &= i(-1)^{A+B} g^2 \sum_{R,S=0}^1 (-1)^{R+S} \int d\xi d\eta t^\alpha \gamma^\mu \\ &\times \mathbf{G}_{AR}(x, \xi) \Gamma_{RB,S}^{d,\lambda}(\xi, y; \eta) \mathbf{D}_{SA,\lambda\mu}^{da}(\eta, x). \end{aligned} \quad (2.9)$$

This formula implies that both quark and gluon correlators,  $\mathbf{G}_{AR}$  and  $\mathbf{D}_{SA,\lambda\mu}^{da}$ , are averaged with the density matrix  $\rho_{\text{in}}$  given by Eq. (2.6). In the first approximation we may replace the exact  $qgg$  vertex by the bare one. Then Eq. (2.8) takes the following simple form:

$$\begin{aligned} \Pi_{AB}^{\mu\nu}(x, y) &= i(-1)^{A+B} g_r^2 \sum_{R,S=0}^1 (-1)^{R+S} \left[ - \int d\xi d\eta \gamma^\mu \mathbf{G}_{AR}(x, \xi) \Gamma_{RS,B}^\nu(\xi, \eta; y) \mathbf{G}_{SA}(\eta, x) \right. \\ &\left. + \int d\xi d\eta V_{acf}^{\mu\alpha\nu}(x, \xi, \eta') \mathbf{D}_{AR}^{cc',\alpha\beta}(\xi, \xi') \mathbf{V}_{RSB;bc'f'}^{\nu\beta\sigma}(\xi', \eta, y) \mathbf{D}_{SA}^{f'f,\lambda\sigma}(\eta, \eta') \right], \end{aligned} \quad (2.13)$$

and we postpone its further expansion because of the complexity of the emerging polarization structure. However, the main idea remains the same as for quark production: in first approximation we get a product of two-quark,  $\mathbf{G}_{01}^{(A)} \mathbf{G}_{10}^{(B)}$ , or two-gluon,  $\mathbf{D}_{01}^{(A)} \mathbf{D}_{10}^{(B)}$  correlation functions. Each of them is averaged with the density matrix of only one of the two nuclei. This is in line with the independence of the initial states of the colliding nuclei.

In a previous paper [5], it was demonstrated how the technique of QFK works at the later (quasi)thermal stages of the heavy-ion collision. It was applied to the problem of dilepton emission from the nonequilibrium quark-gluon plasma (QGP). The technique allows one to examine the balance between real processes and radiative corrections providing proper cancellation of the infrared divergencies at the intermediate stage of calculations (for further details see Ref. [19]).

The explicit form of calculations at the transient stage, conversion of the initial flux of the quarks and gluons into continuous quark-gluon matter, the QGP, is not yet clear. It seems well established that this stage will be dominated by the gluon dynamics: the gluons are most abundant and have the highest rate of interaction. However, there remain some problems to be solved before practical calculation can be carried out. These problems are (i) choice of the initial scale for the structure functions (known as the factorization scale) and (ii) the problem of gauge invariant calculations. The first problem seems to find natural solution in the QFK approach

$$\begin{aligned} p^0 \frac{dN_g}{d\mathbf{p} d^4x} &= \frac{g^2}{2(2\pi)^3} \int \frac{d^4k}{(2\pi)^4} \{ \text{Tr}[(\not{p} + m) t^\alpha \gamma^\mu \\ &\times \mathbf{G}_{01}^{(A)}(p-k) t^\beta \gamma^\mu \mathbf{D}_{10,\nu\mu}^{(B)ba}(-k)] \\ &+ [(A) \leftrightarrow (B)] \}, \end{aligned} \quad (2.10)$$

where the additional superscript (A) or (B) denotes that the correlation function is averaged over the initial state of nucleus A or B, respectively.

A similar procedure yields the following expression for the inclusive gluon production:

$$\frac{dN_g}{d\mathbf{p}} = \sum_{\lambda,a} \int d^4x d^4y \frac{e^{-ip(x-y)}}{(2\pi)^3 2p^0} \epsilon_\mu^{(\lambda)} \epsilon_\nu^{(\lambda)} [-i \Pi_{aa}^{01,\mu\nu}(x, y)] \quad (2.11)$$

where the primary definition of the gluon polarization tensor  $\Pi_{01}$  is given by

$$\Pi_{01,ab}^{\mu\nu}(x, y) = i \left\langle \frac{\delta S^\dagger}{\delta B_\mu^b(y)} \frac{\delta S}{\delta B_\nu^a(x)} \right\rangle. \quad (2.12)$$

Its general formula was derived in [5]:

(see Sec. V). The second problem is not yet solved. It is clear that one should choose a physical gauge. Otherwise one would have to introduce an auxiliary distribution of ghosts which is ill defined. It seems expedient to calculate only the observables, like the energy-momentum tensor, which are gauge invariant. There were many attempts to derive a kind of kinetic equation for the Wigner distributions, which, however, were never successful. At the moment, we connect a hope to overcome this problem with the natural gauge of the ‘‘wedge form’’ of dynamic: the local temporal axial gauge.

### III. DEEP INELASTIC SCATTERING ON THE ELECTRON

In the previous section we have expressed the cross sections of the one-quark and one-gluon production via certain field correlators of the colliding nuclei. The goal of this and the next sections is to find those elements of a theory which are common to two essentially different problems, viz., nucleus-nucleus (or proton-proton) collisions and deep inelastic electron-proton scattering. Our primary demand is that these elements should appear as a by-product of the two independent lines of calculation, initiated separately from first principles. Thus our next step will be a separate investigation of the deep inelastic scattering of the proton on the structureless electron.

We divide this section into two parts. For the sake of completeness we begin with a brief definition of the DIS

cross section in terms of the QFK approach and define the null-plane variables which will be used for all following calculations. Before turning to a detailed derivation of the self-consistent equations in the next section, we give an instructive example of the lowest-order calculations. These have no direct physical value, but they allow one to overcome technical problems and avoid premature discussion of the highly nontrivial approximations.

### A. Basic definitions for DIS

As was emphasized in the Introduction, it is important to have similar definitions of observables for all processes which will participate in the future information exchange. We may rewrite Eq. (2.3) for the inclusive amplitude of DIS as

$$\langle X|a(\mathbf{k}')Sa^\dagger(\mathbf{k})|in\rangle, \quad (3.1)$$

where  $k$  and  $k'$  are the laboratory frame momenta of the electron before and after the scattering. If  $q = k - k'$  is the spacelike momentum transfer, then the DIS cross section is given by

$$k'_0 \frac{d\sigma}{d\mathbf{k}'} = \frac{i\alpha}{(4\pi)^2} \frac{L_{\mu\nu}(k, k')}{(kP)} \frac{W^{\mu\nu}(q)}{(q^2)^2}, \quad (3.2)$$

where  $W^{\mu\nu}(q)$  is the standard Bjorken notation for the correlator of two electromagnetic currents,

$$W^{\mu\nu}(q) = \frac{2V_{\text{lab}}P^0}{4\pi} [-i\pi_{10}^{\mu\nu}(q)]. \quad (3.3)$$

We accept without any discussion its standard tensor decomposition,

$$W^{\mu\nu}(q) = e^{\mu\nu} \frac{\nu W_L}{2x_{Bj}} + \zeta^{\mu\nu} \frac{\nu W_2}{2x_{Bj}M^2}, \quad (3.4)$$

where  $\nu = qP$ ,  $Q^2 = -q^2 > 0$ ,  $x_{Bj} = Q^2/2\nu$ , and

$$e^{\mu\nu} = -g^{\mu\nu} + \frac{q^\mu q^\nu}{q^2},$$

$$\zeta^{\mu\nu} = -g^{\mu\nu} + \frac{P^\mu q^\nu + q^\mu P^\nu}{\nu} - q^2 \frac{P^\mu P^\nu}{\nu^2}. \quad (3.5)$$

Hereafter we will perform all computations using the infinite momentum frame fixed by the null-plane vector  $n^\mu$ ,

$$n^\mu = (1, \mathbf{0}_t, -1), \quad n^2 = 0. \quad (3.6)$$

It defines the “+” components of the Lorentz vectors,

$$na = a^+ = a_- = a^0 + a^3, \quad a^- = a_+ = a^0 - a^3.$$

In the infinite momentum frame, the four-vector of the proton's momentum has components

$$P^\mu = (P^+/2, \mathbf{0}_t, P^+/2), \quad P^- = P^0 - P^3 = 0. \quad (3.7)$$

The momentum transfer has the components

$$q^\mu = (\nu/P^+, \mathbf{q}_t, -\nu/P^+), \quad q^+ = 0, \quad q^- = 2\nu/P^+. \quad (3.8)$$

Instead of the invariant  $W_2$ , we will use the mass-independent structure function  $F_2(x_{Bj}, Q^2) = \nu W_2/M^2$ , which is calculated via the equation

$$c_2 = W^{\mu\nu} n_\mu n_\nu = \frac{(P^+)^2 F_2}{\nu}. \quad (3.9)$$

The longitudinal structure function  $F_L(x_{Bj}, Q^2) = W_L$  should be calculated in accordance with

$$3F_L = 2x_{Bj}c_1 + 2F_2, \quad c_1 = W^{\mu\nu} g_{\mu\nu}. \quad (3.10)$$

### B. An instructive example: The low-order calculation

In order to proceed with the calculations we must specify the density matrix. We shall begin the physical motivation of our choice by reminding the reader that a widely used approach based on Wilson's operator product expansion (OPE) does not utilize any information about the proton's internal structure. Only the total momentum and the discrete quantum numbers are controlled by sum rules. Indeed, the dynamical equations of QCD contribute only to the singular coefficient functions while the regular operator functions, the averages over the proton's state, remain unknown. We can only decide whether or not to include the high-twist operators in the expansion. The twist-1 operators of the OPE correspond to one-particle matrix elements of the proton's density matrix. Including the twist-2 operators into the OPE would correspond to irreducible two-particle correlations in the density matrix used here.

The system of integral equations which we expect to derive eventually does not require any explicit form of the density matrix either. Nevertheless, it is useful to keep in mind some representation which may serve as a simple reference point. For example, we may choose an artificial exponential form which reproduces the total momentum flux of the proton and allows us to derive the integral equations of the Schwinger-Dyson type [5].

The twist-1 operator functions of the OPE, by their structure, are binary products of quark and gluon fields and to some extent resemble occupation numbers which enter the on-mass-shell correlators. For example, in the statistical ensemble we usually have

$$G_{10}(p) = -2\pi i(\not{p} + m)\delta(p^2 - m^2) \times \{\theta(p_0)[1 - n^{(+)}(p)] - \theta(-p_0)n^{(-)}(p)\}. \quad (3.11)$$

We define matrix elements of our one-particle (twist-1) density matrix by a certain set of field correlators. We assign the superscript “#” to all states in the continuum of free on-mass-shell fields:

$$G_{01}^{\#ij}(p) = -2\pi i\delta_{ij}(\not{p} + m)\theta(\pm p^0)\delta(p^2 - m^2), \quad (3.12)$$

$$D_{01}^{\#ab,\mu\nu}(p) = -2\pi i\delta_{ab}d^{\mu\nu}(p)\theta(\pm p_0)\delta(p^2). \quad (3.13)$$

These states are initially empty and the vacuum correlators  $G_{10,01}^{\#}(p)$  and  $D_{10,01}^{\#}(p)$  represent only on-mass-shell particles in the final states.

The superscript “\*” will label “bounded” states of “valence” quarks and gluons in the initial proton:

$$G^*_{01}(p) = 2\pi i \frac{(2\pi)^3}{V_{\text{lab}}} \frac{1}{3} \delta_{ij} \frac{1}{2} \not{p} \delta(p^2) \delta(\mathbf{p}_t) \theta(p^+) \mathcal{V}(p^+), \quad (3.14)$$

$$G^*_{10}(p) = 0. \quad (3.15)$$

The factors 1/2 and 1/3 correspond to the averaging of the distribution over the quark spin and color, respectively. The factor  $(2\pi)^3/V_{\text{lab}}$  corresponds to the normalization: we consider a flux with one proton in a volume  $V_{\text{lab}}$  per unit time.

Equation (3.14) describes the phenomenological distribution of the “valence” quarks as a function of their light-cone momenta  $p^+$ , while Eq. (3.15) means that there are no “valence” antiquarks within the proton. This approach corresponds to beginning the evolution at a very low scale, and was used by Gluck, Reya, and Vogt [20]. At low  $Q^2$  one probably cannot take the perturbative QCD evolution equations seriously. However, if the parameters that are obtained allow for a good fit to the data, these distributions will work as well as any other. If one starts at a higher scale, one should use Eq. (3.15) in the same form as Eq. (3.14). This approach corresponds to the strategy of the CTEQ [21] or Martin-Roberts-Stirling (MRS) [22] parametrizations. We shall discuss them in more detail at the end of Sec. IV.

In the same way we define the “initial” distribution of “valence” gluons by

$$D^{*ab,\mu\nu}_{10}(p) = -2\pi i \frac{1}{8} \frac{(2\pi)^3}{V_{\text{lab}}} \delta_{ab} \frac{1}{2} d^{\mu\nu}(p) \theta(\mp p_0) \times \delta(p^2) \delta(\mathbf{p}_t) \mathcal{G}(p^+), \quad (3.16)$$

with 1/8 and 1/2 standing for the color and polarization average and where  $d^{\mu\nu}$  is a projector

$$d^{\mu\nu}(p) = -g^{\mu\nu} + \frac{p^\mu n^\nu + n^\mu p^\nu}{p^+}, \quad (3.17)$$

which is a sum over the physical gluon polarizations in the null-plane gauge,  $n^\mu B_\mu^a = 0$ .

The reason for introducing these distributions is to give definite values to the quantum numbers (the charges and the momenta). Their densities are given by

$$j^+ = \int \frac{d^4 p}{(2\pi)^4} \text{Tr} \gamma^+ G_{01}^{*ij}(p) = \frac{1}{V_{\text{lab}}} \int_0^{P^+} dp^+ \mathcal{V}(p^+) = \frac{1}{V_{\text{lab}}} \int_0^1 dx \mathcal{V}(x) \quad (3.18)$$

for the quark’s light-cone charge flux, and by

$$T_q^{++} = -i \int \frac{d^4 p}{(2\pi)^4} \text{Tr} \gamma^+ p^+ G_{01}^{*ii}(p) = \frac{1}{V_{\text{lab}}} \int_0^{P^+} dp^+ p^+ \mathcal{V}(p^+) = \frac{P^+}{V_{\text{lab}}} \int_0^1 dx x \mathcal{V}(x) \quad (3.19)$$

for the  $(++)$  component of the quark energy-momentum tensor. In these equations we have introduced the Feynman variable,  $x = x_F = p^+/P^+$ . The momentum flux density from the gluon component is given by

$$T_g^{++} = -i \int \frac{d^4 p}{(2\pi)^4} (p^+)^2 g_{\mu\nu} D_{01}^{*\mu\nu}(p) = \frac{1}{V_{\text{lab}}} \int_0^{P^+} dp^+ p^+ \mathcal{G}(p^+) = \frac{P^+}{V_{\text{lab}}} \int_0^1 dx x \mathcal{G}(x), \quad (3.20)$$

where  $P^+ \mathcal{V}(p^+) \equiv \mathcal{V}(x)$  and  $P^+ \mathcal{G}(p^+) \equiv \mathcal{G}(x)$ . The initial quark and gluon distributions are normalized in such a way that in aggregate they carry the proton’s total quantum numbers.

Neglecting any corrections to the electromagnetic vertex we may rewrite Eq. (3.13) in the following way:

$$W^{\mu\nu}(q) = e_f^2 \frac{2V_{\text{lab}} P_{\text{lab}}}{4\pi} \times \int \frac{d^4 p}{(2\pi)^4} \text{Tr} \gamma^\mu \mathbf{G}_{10}(p+q) \gamma^\nu \mathbf{G}_{01}(p). \quad (3.21)$$

The off-diagonal quark field correlators in this equation obey integral equations [5] which express them in terms of exact retarded and advanced propagators and sources  $\Sigma_{10;01}$  (the “current” correlators):

$$\mathbf{G}_{01} = \mathbf{G}_{\text{ret}} \overleftarrow{G}_{(0)}^{-1} \mathbf{G}_{01} \overrightarrow{G}_{(0)}^{-1} \mathbf{G}_{\text{adv}} - \mathbf{G}_{\text{ret}} \Sigma_{01} \mathbf{G}_{\text{adv}}. \quad (3.22)$$

The retarded and advanced Green’s functions obey more familiar equations,

$$\mathbf{G}_{\text{ret}} = G_{\text{adv}}^{\text{ret}} + G_{\text{adv}}^{\text{ret}} \Sigma_{\text{ret}} G_{\text{adv}}^{\text{ret}}, \quad (3.23)$$

which allow symbolic solutions

$$\mathbf{G}_{\text{ret}}^{-1} = G_{\text{adv}}^{-1} - \Sigma_{\text{ret}}. \quad (3.24)$$

In the first approximation we may replace the exact retarded and advanced quark Green’s functions,  $\mathbf{G}_{\text{ret}}$  and  $\mathbf{G}_{\text{adv}}$ , by the bare ones that carry the same leading light-cone singularity,

$$G_{\text{adv}}^{\text{ret}}(p) = \frac{\not{p}}{(p^0 \pm i0)^2 - \mathbf{p}^2}. \quad (3.25)$$

Then by virtue of (3.15) Eqs. (3.22) take the following form:

$$\mathbf{G}_{01} = G_{01}^\# + G_{01}^* - G_{\text{ret}} \Sigma_{01} G_{\text{adv}}, \quad (3.26)$$

$$\mathbf{G}_{10} = G_{10}^\# - G_{\text{ret}} \Sigma_{10} G_{\text{adv}}. \quad (3.27)$$

In the lowest order we neglect sources and leave only correlators of the initial fields:

$$W^{\mu\nu}(q) = e_f^2 \frac{2V_{\text{lab}} P_{\text{lab}}}{4\pi} \times \int \frac{d^4 p}{(2\pi)^4} \text{Tr} \gamma^\mu G_{10}^\#(p+q) \gamma^\nu G_{01}^*(p). \quad (3.28)$$

Substituting Eqs. (3.12) and (3.14) and rewriting the  $\delta$  function of the on-mass-shell final state quark as

$\delta_+( (p+q)^2 ) = (1/2\nu)\delta(x-x_{B_j})$ , we get the incredibly simple result of the “naive” parton model:

$$F_2^{(0)}(x_{B_j}) = e_f^2 \int_0^1 dx \delta(x-x_{B_j}) x \mathcal{V}(x). \quad (3.29)$$

In the next approximation we should include the quark fields coming from the quark and antiquark sources,  $\Sigma_{01}$  and  $\Sigma_{10}$ , i.e., the last terms in Eqs. (3.26) and (3.27). The general expression for the quark self-energy matrix is given by Eq. (2.9). Still restricting ourselves to bare vertices and bare tree Green functions we get

$$\begin{aligned} \Sigma_{01}^{*\#}(p) = & -ig^2 C_F \int \frac{d^4 k}{(2\pi)^4} \{ \gamma_\mu \mathbf{G}_{01}^*(k) \gamma_\nu D_{10}^{\#\nu\mu}(k-p) \\ & + \gamma_\mu G_{01}^\#(k) \gamma_\nu \mathbf{D}_{10}^{*\nu\mu}(k-p) \}, \end{aligned} \quad (3.30)$$

$$\Sigma_{10}^{*\#}(p) = -ig^2 C_F \int \frac{d^4 k}{(2\pi)^4} \gamma_\mu \mathbf{G}_{10}^\#(k+p) \gamma_\nu D_{01}^{*\nu\mu}(k). \quad (3.31)$$

The superscript “\*#” means that one of the contributing states belongs to the set of final states, while the other originates from the initial proton.

The gluon correlators obey the following equations:

$$\mathbf{D}_{10} = D_{01}^\# + D_{01}^* - \mathbf{D}_{\text{ret}} \Pi_{10} \mathbf{D}_{\text{adv}}, \quad (3.32)$$

$$\mathbf{D}_{\text{adv}}^{\text{ret}} = D_{\text{adv}}^{\text{ret}} + D_{\text{adv}}^{\text{ret}} \Pi_{\text{adv}}^{\text{ret}} \mathbf{D}_{\text{adv}}^{\text{ret}}. \quad (3.33)$$

In the first approximation, all contributions of the gluon sources,  $\Pi_{10,01}$ , should be dropped along with radiative corrections to the retarded and advanced gluon propagators. The tensor structure of the self-energy may be only of the form

$$\Sigma(p) = \not{p} \sigma_2(p) + \not{p} p^+ \sigma_3(p). \quad (3.34)$$

In all the equations it enters in a single combination,

$$\begin{aligned} \not{p} \Sigma(p) \not{p} &= \not{p} \sigma_1(p) + \not{p} p^2 p^+ \sigma_3(p), \\ \sigma_1(p) &= p^2 \sigma_2(p) + 2(p^+)^2 \sigma_3(p). \end{aligned} \quad (3.35)$$

After a long but routine calculation we find

$$\begin{aligned} i\sigma_1^{*\#}(p) = & -\frac{\pi g^2}{V_{\text{lab}} P^+} P^2 \int_{p^+}^{P^+} \frac{dk^+}{k^+} \delta[(p^+ - k^+)p^- - p_t^2] \\ & \times \frac{k^+}{p^+} \left\{ C_F \frac{z^2 + 1}{1-z} P^+ \mathcal{V}(k^+) \right. \\ & \left. + \frac{2z^2 - 2z + 1}{2} P^+ \mathcal{G}(k^+) \right\}, \end{aligned} \quad (3.36)$$

$$\begin{aligned} i\sigma_2^{*\#}(p) = & \frac{\pi g^2}{V_{\text{lab}} P^+} \int_{p^+}^{P^+} \frac{dk^+}{k^+} \delta[(p^+ - k^+)p^- - p_t^2] \\ & \times \frac{k^+}{p^+} \{ C_F P^+ \mathcal{V}(k^+) + \frac{1}{2}(1-z)P^+ \mathcal{G}(k^+) \}, \end{aligned} \quad (3.37)$$

where  $z = p^+/k^+$ , and the invariants for the antiquark source  $\Sigma_{10}$  do not contain terms with valence distribution  $\mathcal{V}(k^+)$ .

It is now straightforward to find the first correction  $F_2^{(1)}(x_{B_j}, Q^2)$  to the DIS structure function:

$$F_2^{(1)}(x_{B_j}) = e_f^2 \int_0^1 dx \delta(x-x_{B_j}) x \Delta^{(1)} q_f(x). \quad (3.38)$$

It is presented in the same form as the zero-order term, (3.29), with  $\mathcal{V}_f(x) = q_f(x, Q_0^2)$  replaced by

$$\Delta^{(1)} q_f(x, Q^2) = \frac{V_{\text{lab}} P^+}{(2\pi)^3} \int_{Q_0^2}^{Q^2} dp_t^2 \int dp^- p^+ \frac{i\sigma_1^{*\#}(p)}{[p^2]^2}. \quad (3.39)$$

To be consistent with the resonant condition of the measurement, we must require that  $Q^2$  be large enough (formally,  $Q^2 \rightarrow \infty$ ), and that the behavior of the integrand at high  $p_t^2$  guarantees the convergence of the integral. If we substitute (3.36) into the right-hand side (RHS) of (3.39) and perform a residual integration over  $p^-$  using the  $\delta$  function

$$\int dp^- \theta(k^+ - p^+) \frac{\delta[(p^+ - k^+)p^- - p_t^2]}{p^2} = -\frac{1}{k^+ p_t^2}, \quad (3.40)$$

then we easily recover the first approximation of the Altarelli-Parisi equation for the nonsinglet quark structure functions of deep inelastic electron-proton scattering.

In the next order we must iterate Eq. (3.32), including the influence of the source  $\Pi_{01}^{\mu\nu}$  on the gluon field. Cutting the accuracy of calculations in Eq. (2.13) to bare vertices, and neglecting the sources in the internal lines, we get the result

$$\begin{aligned} \Pi_{01}^{*\#\mu\nu}(p) = & ig_r^2 \left\{ \int \frac{d^4 k}{(2\pi)^4} \text{Tr}[\gamma^\mu \mathbf{G}_{01}^*(k) \gamma^\nu G_{10}^\#(k-p) + \gamma^\mu G_{01}^\#(k+p) \gamma^\nu \mathbf{G}_{10}^*(k)] \right. \\ & \left. - \int \frac{d^4 k}{(2\pi)^4} V_{acf}^{\mu\alpha\lambda}(p, k-p, -k) \mathbf{D}_{01,cc'}^{*\alpha\beta}(k) V_{bc'f'}^{\nu\beta\sigma}(-p, p-k, k) D_{10,f'f}^{\#\sigma\lambda}(k-p) \right\}, \end{aligned} \quad (3.41)$$

where a sum over the quark flavor  $f$  is assumed in the first term.

The polarization tensor  $\Pi^{\mu\nu}$  only appears between retarded and advanced propagators:  $[D_{\text{ret}}(p)\Pi(p)D_{\text{adv}}(p)]^{\mu\nu}$ . The latter contain projectors  $d^{\mu\nu}(p)$  which are orthogonal to the four-vector  $n^\mu$ . So of the general tensor only two terms survive:

$$\Pi^{\mu\nu}(p) = g^{\mu\nu}w_1(p) + \frac{p^\mu p^\nu}{p^2}w_2(p). \quad (3.42)$$

Others, like  $p^\mu n^\nu + n^\mu p^\nu$  or  $n^\mu n^\nu$ , will cancel out. Introducing one more projector,

$$\begin{aligned} \bar{d}^{\mu\nu}(p) &= -d^{\mu\rho}(p)d_\rho^\nu(p) \\ &= -g^{\mu\nu} + \frac{p^\mu n^\nu + n^\mu p^\nu}{(np)} - p^2 \frac{n^\mu n^\nu}{(p^+)^2}, \end{aligned} \quad (3.43)$$

which is orthogonal to both vectors  $n^\nu$  and  $p^\mu$ , we find

$$\begin{aligned} iw_1^{*\#}(p) &= -\frac{\pi g^2}{V_{\text{lab}}P^+} p^2 \int_{p^+}^{P^+} \frac{dk^+}{k^+} \delta[(p^+ - k^+)p^- - p_t^2] \frac{k^+}{p^+} \\ &\quad \times \left\{ C_F \frac{1 + (1-z)^2}{z} P^+ \mathcal{V}(k^+) + 2N_c \left[ z(1-z) + \frac{z}{1-z} + \frac{1-z}{z} \right] P^+ \mathcal{G}(k^+) \right\}, \end{aligned} \quad (3.46)$$

$$iw_2^{*\#}(p) = -\frac{\pi g^2}{V_{\text{lab}}P^+} p^2 \int_{p^+}^{P^+} \frac{dk^+}{k^+} \delta[(p^+ - k^+)p^- - p_t^2] \frac{k^+}{p^+} \left\{ 4C_F \frac{1-z}{z} P^+ \mathcal{V}(k^+) + 4N_c z \left( 1 - \frac{z}{2} \right) P^+ \mathcal{G}(k^+) \right\}. \quad (3.47)$$

In accordance with the previous convention, and as a reminder of the approximations involved, the invariants carry superscripts  $*\#$ . These indicate that the invariants are contributed to by one proton's "bound" state and one on-mass-shell final state of a quark or gluon. We hope that the reader is not confused by the absence of other indices like quark color, or indices indicating the type of ordering in the invariants  $w_i$  and  $\sigma_i$ . They can easily be recovered when it is needed. For example,  $w_i$  and  $\sigma_i$  are parts of the self-energy which are summed over the color. So if  $\Pi$  and  $\Sigma$  appear as internal elements in any formula, we must restore the color factors in the following way:

$$\Sigma \rightarrow \Sigma_{ij} = \frac{\delta_{ij}}{3} \Sigma, \quad \Pi \rightarrow \Pi_{ab} = \frac{\delta_{ab}}{8} \Pi.$$

Now we may reconstruct a missing element, viz., the first correction to the gluon structure function,

$$\Delta^{(1)}G(x, Q^2) = \frac{V_{\text{lab}}P^+}{(2\pi)^3} \int_{Q_0^2}^{Q^2} dp_t^2 \int dp^- p^+ \frac{iw_1^{*\#}(p)}{[p^2]^2}, \quad (3.48)$$

which is similar to the correction (3.40) to the quark structure function. In a sequence of approximations it should be added to the "valence" gluon distribution  $\mathcal{G}(x)$ .

If we substitute Eq. (3.46) into (3.48), we immediately obtain the lowest-order approximation of the second GLAP equation for the gluon structure function of deep inelastic electron-proton scattering.

Concluding this section, let us pay special attention to the infrared poles at  $z = 1$ , which originate from

that the invariants  $w_1$  and  $w_2$  can be found from two convolutions,

$$-\bar{d}_{\mu\nu}(p)\Pi^{\mu\nu}(p) = 2w_1(p), \quad n_\mu n_\nu \Pi^{\mu\nu}(p) = \frac{p^2}{(p^+)^2} w_2(p), \quad (3.44)$$

independently of other invariants accompanying the missing tensor structures. The new projector, which includes only two transversal gluon modes, naturally appears in the tensor with a gluon source:

$$[d(p)\Pi(p)d(p)]^{\mu\nu} = -\bar{d}_{\mu\nu}(p)w_1(p) + \frac{(p^+)^2}{p^2} w_2(p)n^\mu n^\nu. \quad (3.45)$$

Now it is easy to find the first approximation for the invariants  $w_1(p)$  and  $w_2(p)$ :

the pinch poles of the gluon correlators in the null-plane gauge. To cure this problem we will proceed following Altarelli and Parisi [10]. We will first shield the IR singularity by introduction of the "plus distributions,"

$$\int_0^1 \frac{f(z)dz}{(1-z)_+} = \int_0^1 \frac{f(z) - f(1)}{1-z} dz,$$

and then modify the end-point behavior in such a way that the first integrals are not changed by radiative corrections. The first integrals are the total flux of the flavor  $f$ ,

$$j_f^+ = -iV_{\text{lab}} \int \frac{d^4p}{(2\pi)^4} \text{Tr} \gamma^+ [\mathbf{G}_{01}^f(p) - \mathbf{G}_{10}^f(p)], \quad (3.49)$$

and the total flux of the light-cone momentum,

$$\begin{aligned} T^{++} &= -iV_{\text{lab}} \int \frac{d^4p}{(2\pi)^4} \left\{ \sum_f \text{Tr} \gamma^+ p^+ [\mathbf{G}_{01}^f(p) + \mathbf{G}_{10}^f(p)] \right. \\ &\quad \left. + (p^+)^2 g_{\mu\nu} \mathbf{D}_{01}^{\mu\nu}(p) \right\}. \end{aligned} \quad (3.50)$$

As follows from Eqs. (3.39) and (3.48), the first radiative corrections to the flavor and momentum fluxes are

$$\begin{aligned} \Delta j_f^+ &= \frac{P^+ V_{\text{lab}}}{(2\pi)^3} \int_0^{P^+} dp^+ \int_{Q_0^2}^{Q^2} dp_t^2 \int dp^- p^+ \\ &\quad \times \left[ \frac{i\sigma_1^{f,01}(p)}{[p^2]^2} - \frac{i\sigma_1^{f,10}(p)}{[p^2]^2} \right] \end{aligned} \quad (3.51)$$

and

$$\Delta T^{++} = \frac{P^+ V_{\text{lab}}}{(2\pi)^3} \int_0^{P^+} dp^+ \int_{Q_0^2}^{Q^2} dp_t^2 \int dp^- (p^+)^2 \times \left\{ \sum_f \left[ \frac{i\sigma_1^{f,01}(p)}{[p^2]^2} + \frac{i\sigma_1^{f,10}(p)}{[p^2]^2} \right] + \frac{iw_1^{01}(p)}{[p^2]^2} \right\}, \quad (3.52)$$

respectively. The superscript “#” is omitted because these equations remain valid beyond the first order approximation. The resulting conditions,  $\Delta j_f^+ = 0$  and  $\Delta T^{++} = 0$ , for the splitting kernels in the leading logarithmic approximation are obvious,

$$\int_0^1 P_{qq}(z) dz = 0, \quad \int_0^1 [zP_{gg}(z) + 2n_f zP_{qg}(z)] dz = 0, \quad \int_0^1 [zP_{gq}(z) + zP_{qq}(z)] dz = 0. \quad (3.53)$$

However, beyond the leading logarithmic approximation (LLA) they may change. One now readily finds an explicit form of the splitting kernels,

$$P_{qq}(z) = C_F \left[ \frac{z^2 + 1}{(1-z)_+} + \frac{3}{2} \delta(1-z) \right], \quad P_{qg}(z) = \frac{z^2 + (1-z)^2}{2}, \quad P_{gq}(z) = C_F \frac{1 + (1-z^2)}{z}, \quad P_{gg}(z) = 2N_c \left[ z(1-z) + \frac{z}{(1-z)_+} + \frac{1-z}{z} + \frac{\beta_0}{4N_c} \delta(1-z) \right], \quad (3.54)$$

where the factor  $\beta_0 = 11 - 2n_f/3$  coincides with the first coefficient of the Gell-Mann-Low function.

#### IV. EVOLUTION OF THE SOURCES

Now we are ready to derive integral equations that govern the field correlators and their sources. Actually, they have already been given above. An examination of the calculations in the previous section shows that we did not sum any series. We were consequently performing a series expansion of the previously derived self-consistent solution of the integral Schwinger-Dyson equations. These are Eqs. (2.9) and (2.13), which define the self-energies via the field correlators, and Eqs. (3.26), (3.27), and (3.32), which define the field correlators via the self-energies. We shall rewrite the last equations in the form

$$\mathbf{G}_{10,01} = G_{10,01}^{\#} - \mathbf{G}_{\text{ret}} \Sigma_{10,01} \mathbf{G}_{\text{adv}}, \quad (4.1)$$

and

$$\mathbf{D}_{10,01} = D_{10,01}^{\#} - \mathbf{D}_{\text{ret}} \Pi_{10,01} \mathbf{D}_{\text{adv}}, \quad (4.2)$$

omitting the \*-labeled terms as they do not contribute to the differential form of the evolution equations. In contrast to the integral evolution equations, the differential equations do not require any information about the initial data. At this point we have not made any approximations.

##### A. Dynamical equations in the leading logarithmic approximation

In order to obtain the equations of the leading logarithmic approximation, which sum up the perturbation series with the leading logarithms, we must consider the vertex operators in Eqs. (2.9) and (2.13) as the bare ones. We must also confine one of the off-diagonal field correlators to the out states in the continuum:

$$\Sigma_{01}(p) = ig^2 C_F \int \frac{d^4 k}{(2\pi)^4} \text{Tr} \{ \gamma_\mu \mathbf{G}_{\text{ret}}(k) \Sigma_{01}(k) \mathbf{G}_{\text{adv}}(k) \gamma_\nu D_{10}^{\#\nu\mu}(k-p) + \gamma_\mu G_{01}^{\#}(k+p) \gamma_\nu [\mathbf{D}_{\text{ret}}(k) \Pi_{10}(k) \mathbf{D}_{\text{adv}}(k)]^{\nu\mu} \}, \quad (4.3)$$

$$\Pi_{01}^{\mu\nu}(p) = -ig_r^2 \left\{ - \int \frac{d^4 k}{(2\pi)^4} \text{Tr} [ \gamma^\mu \mathbf{G}_{\text{ret}}(k) \Sigma_{01}(k) \mathbf{G}_{\text{adv}}(k) \gamma^\nu G_{10}^{\#}(k-p) + \gamma^\mu G_{01}^{\#}(k+p) \gamma^\nu \mathbf{G}_{\text{ret}}(k) \Sigma_{01}(k) \mathbf{G}_{\text{adv}}(k) ] + \int \frac{d^4 k}{(2\pi)^4} V_{acf}^{\mu\alpha\nu}(p, k-p, k) [\mathbf{D}_{\text{ret}}(k) \Pi_{01}(k) \mathbf{D}_{\text{adv}}(k)]_{cc'}^{\alpha\beta} V_{bc'f}^{\nu\beta\sigma}(-p, p-k, -k) D_{10,f'f}^{\#\lambda\sigma}(k-p) \right\}. \quad (4.4)$$

By inspection, these equations reveal an astonishing result—the equations which govern the dynamics of the sources  $\Sigma_{01}$  and  $\Pi_{01}$  of the field correlators  $\mathbf{G}_{01}$  and  $\mathbf{D}_{01}$  have a ladder structure. This result appeared though we did not try to set any momentum or angular ordering of the emission process. Equations (4.3) and (4.4) are identical to the initial system of the Schwinger-Dyson equations (4.1) and (4.2) with the only simplification that the

vertices and the final states are not dressed (some generalizations will be considered in Appendix A). We did not sum any perturbation series. The latter would be necessarily divergent. We *start* from the integral equation which sums this series. This result deserves special discussion. We must answer two questions: (i) what was the physical input; and (ii) what follows from the application of the new method to the well known problem of

DIS, for which the solution was obtained earlier using the operator product expansion (OPE).

A more careful analysis shows that our result is not exactly the same as that of the OPE-based approach. Though we get (up to a quantitatively inessential shift of the singularities) the LLA of the perturbation series which results in the GLAP equations, an important qualitative difference appears. The Feynman tree propagators were replaced by the retarded ones. This change reveals the causal structure of the whole process. The last interaction, which puts a single quark onto its mass shell in the perturbative vacuum, is also the latest in time. In other words, the last interaction results in a collapse of the initial wave function.

So, as a by-product, we have answered an old question [7–9] about the correspondence between the evolutionary scale  $Q^2$  or  $x$  and the temporal scale. The causal space-time structure is contained, *a priori*, in evolution equations like the GLAP equations. It is not necessary to impose it *a posteriori*. The  $x$  ordering is a further consequence of the  $\theta$  functions that allow only for emission into the initially unpopulated continuum. The  $Q^2$  ordering with respect to transverse momentum is not a necessary condition, and we shall discuss it shortly.

What are the practical consequences of this picture? First, in order to find the structure functions of the deep inelastic scattering of a proton off an electron, one should know the intensity of the quark field source  $\Sigma_{01}$  *before* the field interaction with the electron. That is why it does not matter before *what kind* of interaction. The intensities of the sources  $\Sigma$  and  $\Pi$  turn out to be universal functions. Unlike the structure functions of DIS they do not depend on the particular choice of measurement procedure. We can also use this reasoning for  $pp$  and  $AA$  collisions. This leads to the conclusion that, if we wish to use  $e-p$  DIS data for the description of  $p-p$  collision dynamics, we should rely on the sources  $\Sigma$  and  $\Pi$ , rather than the structure functions  $q(x, Q^2)$  and  $G(x, Q^2)$ . Their evolution is only a specific projection of the more complicated dynamic of the sources.

The second consequence is that, after the structure functions  $q(x, Q^2)$  and  $G(x, Q^2)$  of the  $e-p$  DIS are found (simply by fitting data, for example), we do not need their phenomenological interpretation as a parton density in order to apply them to other types of collision. This is an explicit advantage because the well known OPE method, instead of calculating the observable  $e-p$  cross section, computes the imaginary part of the truncated Feynman amplitude of the auxiliary Compton process. The next step is a renormalization group analysis of this definite  $S$ -matrix amplitude. As a result, the power of the method is restricted to one single problem of DIS. Any extension of this method requires parton language.

Indeed, though the cross section of the Drell-Yan pro-

cess is defined by the same (except for the kinematic region) polarization operator as in DIS, it cannot be calculated via the OPE. The difference is that now the operator functions should be averaged over a state with two protons. Feynman propagators which contribute to an auxiliary  $S$ -matrix amplitude do not disappear outside the light cone. For the massless partons, and especially in the infinite momentum frame, this leads to the effective interaction *before* the collision. The factorization theorem [35] may be a remedy, but it requires parton language. At the same time it is clear that protons colliding at high energies are causally independent until the moment of collision.

We shall now show that the above equations (4.3) and (4.4) for the self-energies are equivalent to the well known QCD evolution equations. Indeed, let us rewrite Eqs. (4.3) and (4.4) in terms of their tensor components. Beyond the first order calculations of Sec. III B, we must also take into account radiative corrections to the retarded and advanced Green's functions. The spinor (tensor) structure of  $\Sigma_{\text{ret,adv}}$  ( $\Pi_{\text{ret,adv}}$ ), as is given by Eqs. (3.34) and (3.42), remains unchanged. The solution of the Schwinger-Dyson equations (3.23) and (3.33) for retarded and advanced Green's functions is easily cast in the form

$$\begin{aligned} \mathbf{G}_{\text{ret,adv}}(p) &= \frac{\not{p}}{p^2 - \sigma_1^{R,A}(p)} \\ &\quad - \frac{\not{p}p^+ \sigma_3^{R,A}(p)}{[p^2 - \sigma_1^{R,A}(p)][1 - \sigma_2^{R,A}(p)]}, \\ \mathbf{D}_{\text{ret,adv}}^{\mu\nu}(p) &= \frac{\bar{d}^{\mu\nu}(p)}{p^2 - w_1^{R,A}(p)} + \frac{p^2}{(p^+)^2} \frac{n^\mu n^\nu}{p^2 - w_2^{R,A}(p)}. \end{aligned} \quad (4.5)$$

Introducing the following shorthand notations for the denominators of the propagators of different modes:

$$\begin{aligned} \mathcal{W}_1^{R,A}(p) &= p^2 - w_1^{R,A}(p), & \mathcal{W}_2^{R,A}(p) &= p^2 - w_2^{R,A}(p), \\ \mathcal{S}_1^{R,A}(p) &= p^2 - \sigma_1^{R,A}(p), & \mathcal{S}_2^{R,A}(p) &= 1 - \sigma_2^{R,A}(p), \end{aligned} \quad (4.6)$$

we easily obtain

$$\begin{aligned} G_{\text{ret}}(p) \Sigma_{01}(p) G_{\text{adv}}(p) &= \frac{[\not{p} - \not{p}(p^2/2p^+)] \sigma_1^{01}(p)}{\mathcal{S}_1^R(p) \mathcal{S}_1^A(p)} + \frac{\not{p}}{2p^+} \frac{\sigma_2^{01}(p)}{\mathcal{S}_2^R(p) \mathcal{S}_2^A(p)}, \end{aligned} \quad (4.7)$$

$$\begin{aligned} [D_{\text{ret}}(k) \Pi_{01}(k) D_{\text{adv}}(k)]^{\mu\nu} &= \frac{-\bar{d}^{\mu\nu}(p) w_1^{01}(p)}{\mathcal{W}_1^R(p) \mathcal{W}_1^A(p)} + \frac{[p^2/(p^+)^2] w_2^{01}(p) n^\mu n^\nu}{\mathcal{W}_2^R(p) \mathcal{W}_2^A(p)}. \end{aligned} \quad (4.8)$$

The complete evolution equations are long, and are given in Appendix A along with an analysis of further approximations. Here we write only the leading logarithmic terms which eventually result in the GLAP equations:

$$\begin{aligned} \sigma_1^{01}(p) &= \frac{g_r^2}{(2\pi)^3} \int_{p^+}^{P^+} \frac{dk^+}{k^+} \int d^2 \mathbf{k}_t dk^- \delta[(p^+ - k^+)(p^- - k^-) - (\mathbf{p}_t - \mathbf{k}_t)^2] \\ &\quad \times \left[ -p^2 \frac{k^+}{p^+} \right] \left[ P_{qg} \left( \frac{p^+}{k^+} \right) \frac{k^+ \sigma_1^{01}(k)}{\mathcal{S}_1^R(k) \mathcal{S}_1^A(k)} + P_{gq} \left( \frac{p^+}{k^+} \right) \frac{k^+ w_1^{01}(k)}{\mathcal{W}_1^R(k) \mathcal{W}_1^A(k)} + \dots \right], \end{aligned} \quad (4.9)$$

$$\begin{aligned}
w_1^{01}(p) &= \frac{g_\tau^2}{(2\pi)^3} \int_{p^+}^{P^+} \frac{dk^+}{k^+} \int d^2\mathbf{k}_t dk^- \delta[(p^+ - k^+)(p^- - k^-) - (\mathbf{p}_t - \mathbf{k}_t)^2] \\
&\times \left[ -p^2 \frac{k^+}{p^+} \right] \left[ P_{gq} \left( \frac{p^+}{k^+} \right) \frac{k^+ \sigma_1^{01}(k)}{\mathcal{S}_1^R(k) \mathcal{S}_1^A(k)} + P_{gg} \left( \frac{p^+}{k^+} \right) \frac{k^+ w_1^{01}(k)}{\mathcal{W}_1^R(k) \mathcal{W}_1^A(k)} + \dots \right]. \quad (4.10)
\end{aligned}$$

Substituting Eqs. (4.9) and (4.10) into Eqs. (3.9) and (3.21), we easily find that the well known structure functions of the electron-proton deep inelastic scattering are defined by equations which are similar to (3.39) and (3.48):

$$\begin{aligned}
q_f(x, Q^2) &= q_f(x, Q_0^2) + \frac{V_{\text{lab}} P^+}{(2\pi)^3} \int_{Q_0^2}^{Q^2} dp_t^2 \\
&\times \int dp^- \frac{ip^+ \sigma_1^{01}(p)}{\mathcal{S}_1^R(p) \mathcal{S}_1^A(p)}, \quad (4.11)
\end{aligned}$$

$$\begin{aligned}
G(x, Q^2) &= G(x, Q_0^2) + \frac{V_{\text{lab}} P^+}{(2\pi)^3} \int_{Q_0^2}^{Q^2} dp_t^2 \\
&\times \int dp^- \frac{ip^+ w_1^{01}(p)}{\mathcal{W}_1^R(p) \mathcal{W}_1^A(p)}. \quad (4.12)
\end{aligned}$$

The first of these equations is exact; it does not depend on any further approximations. The second one is approximate. It holds only in the LLA. We observe that the structure functions of deep inelastic  $e$ - $p$  scattering in the LLA require only one of the two invariants from each of the sources  $\Pi$  and  $\Sigma$ . This nice feature fails beyond the LLA, and does not hold for processes with different polarization properties of the interaction vertex.

Integration over the null-plane momentum  $p^-$  is a highly nontrivial procedure and it cannot be performed without keeping in mind at least the idea of confinement: before the collision the proton is a composite object and the wave packet which represents it propagates in the physical vacuum without dispersion. When we were doing similar calculations in the lowest order, we designed the density matrix of “valence” quarks and gluons in such a way that  $p^- = 0$  and  $p_t = 0$ . Then they could propagate along the light cone together even without interaction. Now we consider quark and gluon states with  $p_t \neq 0$  and  $p^2 < 0$ , and propagation of these fields before they reach a collision vertex is not free. Assuming the opposite, we would immediately violate the causality principle, or be in contradiction with previous calculations. A partial solution of the problem comes from the vision of the states before the collision as those localized at very small  $\tau$  and at very large rapidity  $y$ . In the wedge form of the dynamic these states, by their design, are predetermined to collapse in the vertex of the interaction. As long as  $p^+ \sim e^y$  and  $p^- \sim e^{-y}$ , and we consider the proton to have infinite positive rapidity, consistency with this limit requires that we put  $p^- = 0$  during all precollision dynamics. On the other hand, the spectral decomposition of the proton in terms of the eigenstates of the wedge dynamic can be viewed as a kind of emission-absorption process. We shall see shortly that the requirement of self-consistency between emission-absorption and propagation provides a natural condition for renormalization.

Suppression of the patterns with  $p^- \neq 0$  in the spectra of the sources is a part of this condition. Physically, it means that the field correlators like  $\Pi(x - y)$  do not depend on the difference  $x^+ - y^+$  of the coordinates in the direction of light-cone propagation. We will conjecture that the exact retarded and advanced propagators indeed protect the wave packet of a proton (or a nucleus) from premature decay, and shall cast the requirement in two forms.

The first, weak form, of this condition can be cast in the form of the inequality  $|k^-| \ll |p^-|$ . Then we may integrate over  $p^-$  using the previous formula (3.40) as a physical approximation. The second, strong form, replaces the inequality by the exact condition  $p^- = 0$ , which can be incorporated into the prescription

$$\frac{ip^+ \sigma_1^{01}(p)}{\mathcal{S}_1^R(p) \mathcal{S}_1^A(p)} = \frac{(2\pi)^3}{V_{\text{lab}} P^+} \delta(p^-) \frac{dq_f(x, p_t^2)}{dp_t^2}, \quad (4.13)$$

$$\frac{ip^+ w_1^{01}(p)}{\mathcal{W}_1^R(p) \mathcal{W}_1^A(p)} = \frac{(2\pi)^3}{V_{\text{lab}} P^+} \delta(p^-) \frac{dG(x, p_t^2)}{dp_t^2}. \quad (4.14)$$

These equations are a recipe on how to use DIS data in the LLA. They require an additional comment about the  $p_t^2$  integration, which is the next step in obtaining the DIS structure functions. First, an unambiguous definition of the structure functions is possible only in the limit of  $\nu \rightarrow \infty$  which eventually leads to the resonant condition (3.38) of the measurement:  $x_F = x_{Bj}$ . Second, when the RHS's of Eqs. (4.9) and (4.10) are integrated over  $p_t^2$  with a large upper limit  $Q^2$ , the kernel of the resulting equation depends on  $k_t^2$  only in the combination  $k_t^2 + (k^+/p^+)Q^2$ . The  $k_t^2$  behavior of the structure function in the new integral should guarantee its convergence. Therefore, one may neglect  $k_t^2$  from the very beginning by assuming that only the domain  $k_t \ll p_t$  contributes in the initial equations. This condition is known as “ordering by angles.” Unlike the ordering by Feynman  $x$ , it is not a fundamental requirement. After integration over  $p_t^2$  in the limit of high  $Q^2$ , the short system (4.9) and (4.10) of the evolution equations results in the GLAP evolution equations for the nonsinglet DIS structure functions [10–12].

The GLAP equations were rederived in a somewhat different way in Refs. [7,23], and with different modifications in Refs. [13–15]. The common element in all these derivations is a selective summation of the divergent perturbation series for the cross section of a specific process in powers of  $\alpha_s \log(Q^2)$  or  $\alpha_s \log(1/x)$  (or both). The only way to obtain a meaningful result is to find an integral equation with an analytic solution that has the same series as its expansion. Depending on which perturbation series is chosen, one obtains the GLAP, BFKL, or Gribov-Levin-Ryskin (GLR) equations.

Our method of obtaining the evolution equation relies neither on the summation of a perturbation series, nor on any particular process we may have in mind. The initial transformation of the Schwinger-Dyson equations of QCD to the form of the solution of the Cauchy problem [5] resulted in a closed system of ladder-type equations which can be reduced to any known evolution equations (after excluding certain types of radiative corrections to propagators and vertices, and high-order correlations).

For example, in the OPE-based approach, the Feynman variable  $x_F$  does not appear at all. Just like the OPE method itself, the GLAP equations are not expected to work at very low  $x$ . Nevertheless, even for low  $x$ , the initial equations (4.9) and (4.10) remain unchanged. In Appendix A, we show that at low  $x$  they may be reduced to the BFKL equation.

An explicit expression for the longitudinal structure function of the DIS follows from Eq. (3.10):

$$3Q^2 F_L(x, Q^2) = \frac{V_{\text{lab}} P^+}{(2\pi)^3} \sum_f e_f^2 \times \int_{Q_0^2}^{Q^2} dp_t^2 \int dp^- \left[ \frac{p^2 \sigma_1(p)}{S_1^R(p) S_1^A(p)} - \frac{\sigma_2(p)}{S_2^R(p) S_2^A(p)} \right]. \quad (4.15)$$

This equation is exact and proves the Callan-Gross relation when we neglect the scaling violation ( $Q^2$  dependence) in the structure functions. The longitudinal structure function found via OPE has an extra small factor  $\alpha_s$ , which is not compensated for by any large logarithm. Thus its contribution to the QCD evolution of the structure function  $F_2$  seems to be small. However, the OPE predictions for  $F_L$  are known to be in poor correspondence with data [25]. In Refs. [26] the  $Q^2$  dependence of  $F_L$  was calculated taking into account the  $k_t$ -dependent gluon distribution. Equation (4.15) provides an excellent opportunity to perform a calculation of  $F_L$  using standard elements of the general evolution scheme.

At present, we can only trace the correspondence between our approximate equations (4.9) and (4.10), and the LLA of the OPE-based calculations or the Lipatov LL(1/ $x$ ) approximation of the Regge calculus. Correspondence between the two approaches in the next orders is still unclear. In what follows we are going to use standard structure functions of the LLA obtained by fitting the data. Thus we shall neglect all terms which can be explicitly reduced to  $F_L$ .

## B. Renormalization of the evolution equations

Until now we have dealt only with objects which do not require renormalization. All these objects were tightly connected with observables. Corresponding field correlators and self-energies were imaginary and for this reason could not contain ultraviolet divergencies. So we could safely use a "naive" form of the Schwinger-Dyson equations,

$$\mathbf{G}_{AB} = G_{AB} + \sum_{RS} G_{AR} \Sigma_{RS} \mathbf{G}_{SB},$$

$$\mathbf{D}_{AB} = D_{AB} + \sum_{RS} D_{AR} \Pi_{RS} \mathbf{D}_{SB}. \quad (4.16)$$

The divergent retarded and advanced self-energies were completely neglected, and retarded and advanced Green's functions were treated as the bare ones. Consequently, the counterterms of the Lagrangian still did not manifest themselves, and the renormalized coupling constant  $g_r$  still remains undefined. We must now fill this gap.

After including the counterterms we obtain the same equations, but with the self-energies modified by the quasilocal terms:

$$\mathbf{D}_{AB} = D_{AB} + \sum_{RS} D_{AR} [(Z_{1F} \Pi'_{RS} + Z_1 \Pi''_{RS}) + (1 - Z_3) (-1)^R \delta_{RS} D_0^{-1}] \mathbf{D}_{SB}, \quad (4.17)$$

$$\mathbf{G}_{AB} = G_{AB} + \sum_{RS} G_{AR} [Z_{1F} \Sigma_{RS} + (1 - Z_2) (-1)^R \delta_{RS} G_0^{-1}] \mathbf{G}_{SB}, \quad (4.18)$$

where  $\Pi'$  and  $\Pi''$  are the fermion and gluon loops, respectively. In perturbative calculations the factors  $Z_{1,1F}$  should be split further as  $Z_{1,1F} = 1 + (Z_{1,1F} - 1)$ , with the second term assigned to the UV renormalization of the vertex. The only changes from Eqs. (4.16) are due to additional *diagonal* terms in  $\Pi$  and  $\Sigma$ . This is quite natural as the off-diagonal terms are imaginary and if they were divergent we would have no remedy. As the matrix structure of Eqs. (4.18) and (4.18) is literally the same as that of Eqs. (4.16), we can rotate the  $2 \times 2$  basis as usual [6,5]. Keeping in mind the light-cone dominance, we may rewrite equations for  $T$ -ordered and  $T^\dagger$ -ordered correlators as

$$\mathbf{D}_{11}^{\#}(p) = D_{11}^{\#}(p) + D_{\text{ret}}(p) [(Z_{1F} \Pi'_{11} + Z_1 \Pi''_{11}) \pm (1 - Z_3) D_0^{-1}(p)] D_{\text{adv}}(p), \quad (4.19)$$

$$\mathbf{G}_{11}^{\#}(p) = G_{11}^{\#}(p) + G_{\text{ret}}(p) [Z_{1F} \Sigma_{11} \pm (1 - Z_2) G_0^{-1}(p)] G_{\text{adv}}(p), \quad (4.20)$$

where  $\Pi_{11,00}(p)$  and  $\Sigma_{11,00}(p)$  should be calculated using Eqs. (2.10) and (2.13) with the bare vertices and no more than one source. We omit the \*-labeled terms here as we are interested in the UV renormalization and low- $x$  effects. These terms are effectively cut off at very high momenta and do not affect the latest stages of evolution.

Equations (4.19) and (4.20) are too approximate to give an explicit value of the running coupling constant. The questions we want to consider are the following: (i) does renormalization of the sources  $\Pi$  and  $\Sigma$  result in renormalization of the coupling constant? and (ii) does

the coupling constant, attached to the vertex at some moment  $t$ , require for its renormalization any information besides the dynamics of the ladder at previous moments?

Before turning to explicit calculations, let us address some qualitative issues. The new equations are not completely independent of those we have already studied. Indeed, the sums and the differences

$$\begin{aligned} D_1 &= D_{00} + D_{11} = D_{10} + D_{01}, \\ \Pi_1 &= \Pi_{00} + \Pi_{11} = -\Pi_{10} - \Pi_{01}, \\ D_0 &= D_{\text{ret}} - D_{\text{adv}} = D_{10} - D_{01}, \\ \Pi_0 &= \Pi_{\text{ret}} - \Pi_{\text{adv}} = -\Pi_{10} + \Pi_{01} \end{aligned} \quad (4.21)$$

define imaginary parts of  $T$ - and  $T^\dagger$ -ordered, as well as retarded and advanced, correlators in an interdependent way. The real parts are not independent either. Indeed,

$$\begin{aligned} 2D_s &= D_{00} - D_{11} = D_{\text{ret}} + D_{\text{adv}} \\ &= 2\text{Re}D_{00} = -2\text{Re}D_{11} = 2\text{Re}D_{\text{ret}} \\ &= 2\text{Re}D_{\text{adv}}, \\ 2\Pi_s &= \Pi_{00} - \Pi_{11} = \Pi_{\text{ret}} + \Pi_{\text{adv}} \\ &= 2\text{Re}\Pi_{00} = -2\text{Re}\Pi_{11} = 2\text{Re}\Pi_{\text{ret}} \\ &= 2\text{Re}\Pi_{\text{adv}}. \end{aligned} \quad (4.22)$$

In addition, the causality principle connects real and imaginary parts of the retarded and advanced correlators by means of dispersion relations. Therefore we can draw two major conclusions: (i) we have to follow the BHPZ scheme [24] in regularization of the divergent real functions, and (ii) the physical condition of renormalization should be consistent with the above analysis of the evolution of the sources. Let us begin by writing down the integral equation for the gluon polarization correlators in the leading approximation:

$$\begin{aligned} \Pi_{00}^{\mu\nu}(p) &= \Pi_{00}^{(0)\mu\nu}(p) - ig_r^2 \int \frac{d^4k}{(2\pi)^4} \text{Tr}[\gamma^\mu G_{00}(k-p) \gamma^\nu G_{\text{ret}}(k) [Z_{1F} \Sigma_{11}(p) + (1-Z_2) G_0^{-1}(k)] G_{\text{adv}}(k) \\ &\quad - ig_r^2 \int \frac{d^4k}{(2\pi)^4} V_{acf}^{\mu\alpha\nu}(p, k-p, -k) D_{00,cc'}^{\alpha\beta}(k-p) V_{bc'f'}^{\nu\beta\sigma}(-p, p-k, k) \\ &\quad \times \{D_{\text{ret}}(k) [(Z_{1F} \Pi'_{11} + Z_1 \Pi''_{11})(k) + (1-Z_3) D_0^{-1}(k)] D_{\text{adv}}(k)\}_{f'f}^{\lambda\sigma}. \end{aligned} \quad (4.23)$$

The corresponding equation for  $\Pi_{11}^{\mu\nu}(p)$  is the complex anticonjugate of Eq. (4.23), and can be obtained via replacement of the  $T$ -ordered functions by the minus  $T^\dagger$ -ordered ones and vice versa. Similar integral equations may be written for the fermion sources. In complete agreement with (4.21) and (4.22), these equations have ladder structure with retarded behavior. To lowest order, gluon and fermion Green functions are given by

$$D_{00}^{\mu\nu}(p) = \frac{\pm d^{\mu\nu}(p)}{p^2 \pm i0}, \quad G_{00}^{\mu\nu}(p) = \frac{\pm \not{p}}{p^2 \pm i0}, \quad (4.24)$$

and  $\Pi_{00}^{(0)\mu\nu}(p)$  is the usual ultraviolet-divergent vacuum gluon polarization tensor.

For the sake of simplicity, let us consider only the gluon sector in the leading approximation. Projecting Eq. (4.24) onto the normal modes, one obtains

$$\begin{aligned} w_1^{00}(p) &= w_{(0)1}^{00}(p) - \frac{iZ_1 g_r^2}{2(2\pi)^4} \int \frac{d^4k}{(k-p)^2 - i0} \mathcal{I}\left(\frac{p^+}{k^+}\right) \\ &\quad \times \frac{w_1^{11}(k) + (1-Z_3)k^2}{[k^2]^2} \end{aligned} \quad (4.25)$$

where we have denoted

$$\mathcal{I}(z) = 8[(-p^2/z + k^2) P_{gg}(z) - (k-p)^2(z + 1/z - 1/4)],$$

and the splitting kernel  $P_{gg}$  is the same as in the evolution equation for a gluon source  $\Pi_{01}$ . It must be IR regularized in the same way, otherwise we would obtain a contradiction with Eqs. (4.21) and (4.22). Alternating  $T$ -ordered and  $T^\dagger$ -ordered correlators in the ladder rungs is crucial for the subsequent conclusions.

The imaginary part of Eq. (4.25) is finite. It can be obtained as the sum of the two ladder equations for  $w_1^{01}$  and  $w_1^{10}$ . The divergent real part of the equation in the leading approximation is an equation for  $\text{Re}w_1^{00} = \text{Re}w_1^R$ , i.e., the real part of the retarded self-energy. Separating real and imaginary parts in Eq. (4.25) one obtains

$$\begin{aligned} w_1^s(p) &= w_{(0)1}^s(p) + \frac{Z_1 g_r^2 N_c}{2(2\pi)^3} \left[ \int d^4k \delta[(k-p)^2] \mathcal{I}\left(\frac{p^+}{k^+}\right) \right. \\ &\quad \times \frac{w_1^s(k) + (1-Z_3)k^2}{[k^2]^2} \\ &\quad \left. + \frac{i}{2\pi} \int d^4k \frac{\mathcal{P}}{(k-p)^2} \mathcal{I}\left(\frac{p^+}{k^+}\right) \frac{w_1^1(k)}{[k^2]^2} \right], \end{aligned} \quad (4.26)$$

where  $\mathcal{P}$  denotes principal value integration. Another way to derive this equation is to start with the explicit expression for the retarded self-energy. Their sum, being projected onto the transverse normal mode, leads again to Eq. (4.26). This consistency is a consequence of the dispersion relation for  $\Pi_{\text{ret}}$  which allows one to recover  $\text{Re}\Pi_{\text{ret}}$  via the already known  $\text{Im}\Pi_{\text{ret}}$ . It reassures us that we are considering the propagation of the gluon field in agreement with the precollision dynamics of the sources.

Indeed, the explicit expression for the retarded and advanced gluon self-energies can be written as

$$\begin{aligned} \Pi_{\text{adv}}^{\mu\nu}(p) &= ig_r^2 \int \frac{d^4k}{(2\pi)^4} V_{acf}^{\mu\alpha\lambda}(p, -k-p, k) D_{\text{adv}}^{cc',\alpha\beta}(k+p) \\ &\quad \times V_{bc'f'}^{\nu\beta\sigma}(-p, p+k, -k) D_1^{f'f,\sigma\lambda}(k). \end{aligned} \quad (4.27)$$

This equation has a very clear physical meaning. The propagator in the loop is retarded (advanced), and guarantees the required time direction. It is affected by the surroundings less than other correlators. The correlator  $D_1$  describes the density of states which develops in the course of the evolution. Thus, even the light-cone propagation is not really free—emission introduces additional phase shifts which result in the assembly of special wave packets.

One may easily see that the imaginary part of the self-energy, considered given, defines the free term in the inhomogeneous equation (4.26) for the real part of the gluon self-energy. The unusual feature of this equation [which is common for all ladder-type equations like (4.23)] is the counterterm which is detached from the vacuum part of the self-energy. The latter is divergent, and the corresponding counterterm is in the integrand of the equation. This immediately requires that the kernel should act on the counterterm as  $\delta(k-p)$ . Furthermore, the integral which contains the counterterm, by inspection, is proportional to the one-loop vacuum self-energy of a gluon. After the UV renormalization, the latter typically behaves like  $p^2 \ln(p^2/\Lambda^2)$ , where  $\Lambda$  is the IR cut-off mass. We find that in order to have the counterterm  $-p^2(1-Z_3)$  in its legitimate place near  $w_{(0)1}^s(p)$ , the following relation should hold:  $\alpha_r \sim 1/\ln(p^2/\Lambda^2)$ .

We have estimated the contribution of the counterterm by first calculating the imaginary part of the retarded gluon self-energy, and then singling out the logarithmic terms in the dispersion integral for the real part. We obtained

$$\alpha_r(p_t^2) = \frac{4\pi}{\beta_0 \ln(p_t^2/\Lambda^2)}. \quad (4.28)$$

Thus the known behavior of the running coupling constant is recovered. Since we have used very rough approximations, the exact equality of the coefficient deserves further study. In the renormalization group approach it is a direct consequence of the Slavnov-Taylor identity in the null-plane gauge:  $Z_1 = Z_3$ . After this renormalization the integral equation (4.26) for the real part of the gluon self-energy  $[w_1^s(p)]^{\text{ren}}$  takes its final shape:

$$\begin{aligned} w_1^s(p) &= w_{(0)1}^s(p) + \frac{\alpha_s(p_t^2)N_c}{(2\pi)^2} \int d^4k \delta[(k-p)^2] \mathcal{I} \left( \frac{p^+}{k^+} \right) \\ &\times \frac{w_1^s(k)}{[k^2]^2} + i \frac{\alpha_s(p_t^2)N_c}{(2\pi)^3} \int d^4k \frac{\mathcal{P}}{(k-p)^2} \\ &\times \mathcal{I} \left( \frac{p^+}{k^+} \right) \frac{w_1^s(k)}{[k^2]^2}, \end{aligned} \quad (4.29)$$

where the superscript “ren” is omitted.

Despite the remaining uncertainty caused by the approximation, it seems to be very important that the running coupling appears as a consequence of causal evolution. Only the processes which took place inside the past light cone of the local interaction contribute to the magnitude of the coupling in its vertex. This guarantees the proper balance between propagation and emission-absorption processes at the precollision stage.

We still have freedom to choose  $Z_3$ . It has not yet been used in the renormalization; the running coupling has appeared as a necessary condition for renormalization rather than as an explicit choice of some physical parameters at some given four-momentum. The strategy behind this choice must be the same as in the old-fashioned on-mass-shell renormalization of the asymptotic state: the on-mass-shell property means that the field propagation is steady, despite background vacuum fluctuations. Selecting this kind of boundary condition, we cannot describe the dynamics which leads to the “undressing” of the quark as required by the resonant condition of deep inelastic scattering. Moreover, the imaginary part of the self-energy must equal zero at the renormalization point.

Thus the object we now study is a field configuration which has quite different properties from those of a free particle. This is evident, for example, from Eq. (4.14), which indicates that the imaginary part of  $w_1^R(p)$  is strongly peaked near  $p^- = 0$ . This configuration is singled out by two requirements (boundary conditions): (i) at the end of its evolution, it produces an off-shell quark that can interact with the electron in a resonant way; (ii) this quark stays bare (on shell) after the scattering.

In  $e-p$  deep inelastic scattering the second condition does not look too realistic. The bare quark will immediately fragment into a hadronic jet. In  $p-p$  collisions, the electron is replaced by a gluon from the second proton, but the final quark state must still propagate in the physical vacuum and decays into hadrons as well. Only in  $AA$  collisions do we expect the creation of a volume of perturbative vacuum large enough to allow almost stable free propagation.

The most important point is that the precollision dynamics of the field fluctuations is the same in all three cases. This is guaranteed by the geometry of the high-energy collision and the causality principle. However, one should keep in mind that the types of fluctuations studied by DIS are strictly selected by the trigger of the specific measurement. Imposing other triggers will select other types of fluctuations. It cannot be ruled out *a priori* that the pieces  $w_2$  and  $\sigma_2$  that were neglected in the LLA may become more significant.

To find an analogy between the precollision dynamics of the proton constituents and the physics of continuous media, we may try to associate components of gluon self-energy with the electromagnetic susceptibility. If its imaginary part is infinite then we have an ideally conducting medium. (Remember that  $p^-$  is a “frequency” corresponding to the “time”  $x^+$ .) A significant growth of the imaginary part of the self-energy at the “resonance”  $p^- = 0$  should lead to anomalous dispersion—the real part must drop to zero:

$$\text{Re} w_1^R(p_t^2, p^+, p^- = 0) - (1 - Z_3)(-p_t^2) = 0. \quad (4.30)$$

[We can suggest the formal mathematical argument: once  $\text{Im} \Pi_{\text{ret}} \sim \delta(p^-)$ , then from the dispersion relation  $\text{Re} \Pi_{\text{ret}} \sim \mathcal{P}(1/p^-)$  which, though in a singular manner, is equal to zero at  $p^- = 0$ .] In the region of anomalous dispersion, the phase and the group velocities should have opposite signs. This reveals one more unusual feature of

the “undressing” process: the phases of the fields participating in the assembly of the wave packet representing an interacting quark (or gluon) travel in the “normal” time direction (from the past to the future). These fields leave “holes” in the sea. Only the act of measurement (scattering) transforms the creation of these “holes” into the process of multiple emission.

### C. Several remarks about the DIS data and the parametrization of the structure functions

The analysis of the evolution equations in this and previous sections had the goal of finding those elements of the theory which are common for the two different processes, viz., deep inelastic  $e$ - $p$  scattering, and high-energy hadronic or nuclear collisions. These elements are the sources. They enter the cross sections of hadronic processes and the DIS structure functions on an equal footing. The only significant difference is that the longitudinal components of the quark sources do not contribute to the structure function  $F_2$  directly. They do contribute to  $F_L$ , but the importance of this function is commonly considered to be secondary. The  $F_L$  function is difficult to obtain from data. Though it is directly affected by the gluon distribution, the corresponding information is almost never used in parametrization of the structure functions.

Any known set of structure function parametrizations, e.g., Gluck-Reya-Vogt (GRV) [20], CTEQ [21], or MRS [22], is equally good for the calculation of hadronic processes in the domain where they fit the data properly. Unfortunately, the DIS data are not available in a wide enough region, and any of the sets usually requires corrections when a new range of  $x$  or  $Q^2$  is measured.

The new low- $x$  data from HERA [27,28] are seriously challenging the current parametrizations. The first analysis of the 1993 ZEUS data [27] indicates that at  $x_{Bj} < 10^{-2}$  and  $8.5 < Q^2 < 30 \text{ GeV}^2$  the data favor the CTEQ2D' parametrization. For  $30 < Q^2 < 125 \text{ GeV}^2$  the MRSD is better, while at larger  $Q^2$  and larger  $x_{Bj}$  both distributions are equally good. Notice, however, that the 1993 HERA data are already accounted for in the MRS parametrization of 1994.

The 1993 ZEUS data seem to be in poor agreement with the GRV(HO) calculations, but a systematic improvement of the correspondence is obtained when the GRV calculations at  $x_{Bj} < 10^{-2}$  are modified to take into account the  $c$ -quark mass and threshold effects according to Refs. [29,30]. In these papers, the heavy quark was considered as a product of the process  $ep \rightarrow c\bar{c}X$ , rather than as a constituent of the QCD evolution. At  $Q^2 \gg m_c^2$  the latter is more reasonable.

A smoother description of the transient regime in the vicinity of the threshold  $Q^2 = m_c^2$  was suggested in Refs. [31,32]. In these calculations, various regions (below and above the threshold) were treated in a different manner: with different numbers of active flavors, and different renormalization prescriptions. Special subtraction schemes were introduced at the threshold.

Clearly, at very large  $Q^2$ , all four (or five) quark flavors,

along with the gluons, uniformly participate in QCD evolution. The definition of the heavy flavor DIS structure functions (or sources) should be identical to those of gluons and light sea quarks. Only in this way can one consistently introduce the notion of intrinsic charm and beauty, and describe their excitations unambiguously. The contribution of heavy flavors should naturally die out when we move in the direction of lower  $Q^2$  along the evolution scale. An inspection of the evolution equations (4.9) and (4.10) extended to finite quark masses indicates that they have a good chance of providing this kind of uniform description (work in progress).

We do not discuss the theory of hadronic and nuclear shadowing and the corresponding data. There were several attempts to incorporate these data into the calculations of charm production [33,34]. However, the current status of nuclear shadowing theory remains controversial.

## V. DISTRIBUTIONS OF QUARKS AND GLUONS IN LEADING ORDER

In this and the following sections we present results of an explicit calculation of the single-particle distribution of light quarks and gluons produced at the earliest stage of an  $AA$  collision. In this section we calculate cross sections to the lowest order. It is general practice to associate the corresponding processes with the excitation of sea quarks and gluons. There are three processes of this type. Their graphs are shown in Fig. 1. In Sec. VI we will derive a complete set of equations for the first order processes, and discuss how one avoids difficulties that accompany calculations based on the factorization theorem [35].

### A. Production of light quarks to leading order

We return to the initial formulas (2.8) and (2.10), and rewrite the former in the momentum representation:

$$\frac{dN_q}{dpd^4x} = \frac{\text{Tr}[i\hat{p}\Sigma_{01}^{ii}(p)]}{(2\pi)^3 2p^0}. \quad (5.1)$$

The lowest order of our theory assumes that: (i) the exact

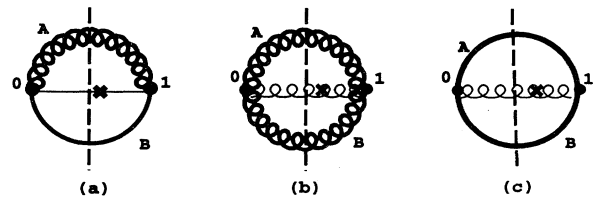


FIG. 1. Born diagrams for one-quark and one-gluon production. The bold cross labels the line corresponding to the “detected” particle with momentum  $p$ . The dashed line crosses the field correlators representing densities of the initial (bold) or final (thin) states. Numbers near the vertices indicate the type of ordering in the field correlators. The processes: (a)  $qg \rightarrow q$ ; (b)  $gg \rightarrow g$ ; (c)  $q\bar{q} \rightarrow g$ .

vertex operator must be replaced by the bare one, which leads to

$$p^0 \frac{dN_q}{d\mathbf{p}d^4x} = \frac{g^2}{2(2\pi)^3} \int \frac{d^4k}{(2\pi)^4} \times \text{Tr}[\not{p}t^a \gamma^\mu \mathbf{G}_{01}(p+k)t^b \gamma^\mu \mathbf{D}_{10,\nu\mu}^{ba}(k)]; \quad (5.2)$$

and (ii) in  $\mathbf{G}_{01}$  and  $\mathbf{D}_{10}$ , possible contributions of the out states of quarks and gluons in the continuum are excluded. These contributions are described by the higher orders of perturbation theory. Thus, we naturally arrive at Eq. (2.10),

$$p^0 \frac{dN_q}{d\mathbf{p}d^4x} = \frac{g^2}{2(2\pi)^3} \int \frac{d^4k d^4q}{(2\pi)^4} \delta(k+q-p) \times \{ \text{Tr}[\not{p}t^a \gamma^\mu \mathbf{G}_{01}^{(B)}(q)t^b \gamma^\mu \mathbf{D}_{01,\nu\mu}^{(A)ba}(k)] + [(A) \leftrightarrow (B)] \}, \quad (5.3)$$

where the quark and gluon correlators must be taken in the following form:

$$\begin{aligned} \mathbf{G}_{01}^{(J)} &= G_{01}^{*(J)} - \mathbf{G}_{\text{ret}}^{(J)} \Sigma_{01}^{(J)} \mathbf{G}_{\text{adv}}^{(J)}, \\ \mathbf{D}_{01}^{(J)} &= D_{01}^{*(J)} - \mathbf{D}_{\text{ret}}^{(J)} \Pi_{01}^{(J)} \mathbf{D}_{\text{adv}}^{(J)} \quad (J = A, B), \end{aligned} \quad (5.4)$$

with  $G_{01}^{*(J)}$  and  $D_{01}^{*(J)}$  representing the quark and gluon distributions, respectively, at some arbitrary scale  $Q_0^2$ . For computations, we shall use a standard CTEQ parametrization of the nucleon structure functions [21]  $q(x, q_t^2)$  and  $G(x, k_t^2)$ . These were obtained by fitting the data with the solutions of the GLAP evolution equations. For nuclei, we shall also use the semiempirical formula fitted to nuclear shadowing data.

We proceed in the laboratory frame, which is the infinite momentum frame for both proton  $A$  and proton  $B$ . The directions of their light-cone propagation are fixed by the two null-plane vectors  $n_A^\mu$  and  $n_B^\mu$ :

$$n_A^\mu = (1, \mathbf{0}_t, -1), \quad n_B^\mu = (1, \mathbf{0}_t, 1), \quad n_A^2 = n_B^2 = 0. \quad (5.5)$$

They define the light-cone components of the Lorentz vectors:

$$n_A a = a^+ = a_- = a^0 + a^3, \quad n_B b = b^- = b_+ = b^0 - b^3.$$

We split the total cross section into three parts:

$$\sigma_q^{(0)} = \sigma_q^{(0)}(\mathcal{V}, \Pi) + \sigma_q^{(0)}(\mathcal{G}, \Sigma) + \sigma_q^{(0)}(\Pi, \Sigma). \quad (5.6)$$

The term  $\sigma_q^{(0)}(\mathcal{G}, \mathcal{G})$  is naturally absent, as energy-momentum conservation prevents fusion of the two on-mass-shell particles into one on-mass-shell quark.

Unlike the case of DIS, both the invariants from quark ( $\sigma_1$  and  $\sigma_2$ ) and gluon ( $w_1$  and  $w_2$ ) self-energies contribute to the cross section of quark production. In order not to exceed the accuracy of the leading logarithmic approximation of the GLAP evolution of structure functions, we shall omit  $\sigma_2$  and  $w_2$ . They are of the next order by a formal count of the  $\alpha_s$  powers, and are not under direct control of DIS data.

Any term coming from the nucleus  $A$  carries a  $\delta(k^-)$ , and any term coming from the nuclei  $B$  carries a  $\delta(q^+)$ . This drastically simplifies the calculation. The first two terms from Eq. (5.6) are calculated explicitly, yielding

$$\frac{d\sigma_q^{(0)}(\mathcal{V}, \Pi)}{dp_t^2 dy} = \frac{16\pi^2 \alpha_0}{3s} \left[ q \left( \frac{p_t e^{-y}}{\sqrt{s}}, Q_0^2 \right) G' \left( \frac{p_t e^y}{\sqrt{s}}, p_t^2 \right) + (y \rightarrow -y) \right], \quad (5.7)$$

$$\frac{d\sigma_q^{(0)}(\mathcal{G}, \Sigma)}{dp_t^2 dy} = \frac{16\pi^2 \alpha_0}{3s} \left\{ G \left( \frac{p_t e^{-y}}{\sqrt{s}}, Q_0^2 \right) q' \left( \frac{p_t e^y}{\sqrt{s}}, p_t^2 \right) \times \left[ 1 + \frac{p_t^2}{s x_A x_B} \right] + (y \rightarrow -y) \right\}, \quad (5.8)$$

where  $y$  is the longitudinal rapidity of the final state quark,  $x_{A,B} = p_t e^{\pm y} / \sqrt{s}$ , and the substitute term ( $y \rightarrow -y$ ) accounts for the symmetry ( $A \leftrightarrow B$ ). We have also defined  $G'(x, p_t^2) = dG(x, p_t^2) / dp_t^2$  and  $q'(x, p_t^2) = dq(x, p_t^2) / dp_t^2$ . The main contribution to the cross section comes from the third term in Eq. (5.6):

$$\begin{aligned} \frac{d\sigma_q^{(0)}(\Sigma, \Pi)}{dp_t^2 dy} &= \frac{8\pi \alpha_0}{3s p_t^2} \int \frac{dk_t^2 dq_t^2 (k_t^2 + q_t^2) (1 + q_t^2 / s x_A x_B)}{\sqrt{[(k_t + q_t)^2 - p_t^2] [p_t^2 - (k_t - q_t)^2]}} \\ &\times \left[ q' \left( \frac{p_t e^{-y}}{\sqrt{s}}, q_t^2 \right) G' \left( \frac{p_t e^y}{\sqrt{s}}, k_t^2 \right) + (y \rightarrow -y) \right], \end{aligned} \quad (5.9)$$

where all terms which are at least as small as the longitudinal structure function  $F_L$  of the DIS are neglected. The square root in the denominator comes from the angular integration over the orientations of the transverse momenta:

$$\begin{aligned} \int d^2 \mathbf{k}_t d^2 \mathbf{q}_t \delta^{(2)}(\mathbf{k}_t + \mathbf{q}_t - \mathbf{p}_t) F(k_t, q_t) \\ = \int \frac{dk_t^2 dq_t^2 F(k_t, q_t)}{4S(k_t, q_t, p_t)}, \end{aligned} \quad (5.10)$$

where  $S(k_t, q_t, p_t)$  is the area of the triangle with sides  $k_t$ ,  $q_t$ , and  $p_t$ ,

$$4S(k_t, q_t, p_t) = \sqrt{[(k_t + q_t)^2 - p_t^2] [p_t^2 - (k_t - q_t)^2]}, \quad (5.11)$$

and the integration domain is restricted by the triangle inequalities

$$k_t + q_t \geq p_t, \quad |k_t - q_t| \leq p_t. \quad (5.12)$$

### B. Production of gluons to leading order

For the case of gluon production, we start from Eq. (2.11), and, as for Eq. (5.1), rewrite it in the momentum representation:

$$\frac{dN_g}{d\mathbf{p}d^4x} = \frac{d_{\mu\nu}(p, u)[-i\Pi_{01}^{\alpha\alpha, \mu\nu}(p)]}{(2\pi)^3 2p^0}, \quad (5.13)$$

where the projector  $d_{\mu\nu}(p, u)$

$$d^{\mu\nu}(p, u) = -g^{\mu\nu} + \frac{p^\mu u^\nu + u^\mu p^\nu}{(pu)} - \frac{p^\mu p^\nu}{(pu)^2},$$

$$d^{\mu\nu}(p, u)u_\nu = 0, \quad p^2 = 0, \quad (5.14)$$

is a sum over the two physical gluon polarizations in the laboratory frame with the time axis along the four-vector  $u^\mu = (1, 0, 0, 0)$ . For this gluon we choose the timelike axial gauge  $u^\mu B_\mu^\alpha = 0$ ,  $u^2 = 1$ . This particular choice of the gauge for the final state gluon should be considered as an example only. The gauge independence of the cross sections with the off-mass-shell initial states of the gluons is a nontrivial question which will be discussed later in a separate paper. Practically, the problem is solved by the choice of an exotic gauge condition,  $A^\tau = 0$ , where  $A^\tau$  is the component of the gluon field along the normal to the hypersurface  $\tau = \text{const}$ .

To the same approximation as in Eq. (5.2), we may write the gluon polarization tensor (temporarily omitting the fermion contribution) as

$$\begin{aligned} \Pi_{01}^{\mu\nu}(p) = & -ig_0^2 \int \frac{d^4k d^4q}{(2\pi)^4} \delta(k+q-p) V_{acd}^{\mu\rho\sigma}(k+q, -q, -k) \mathbf{D}_{01, dd'}^{(A)\sigma\beta}(k) V_{bc'd'}^{\nu\lambda\beta}(-k-q, q, k) \\ & \times \mathbf{D}_{10, f'f}^{(B)\rho\lambda}(q) + (A \leftrightarrow B). \end{aligned} \quad (5.15)$$

The gluon distribution of each nucleus consists of the two familiar terms given by Eq. (5.4). Again, we shall keep only the leading terms in the gluon sources which are under the control of the data:

$$[d(k, n_A) \Pi^{(A)}(k) d(k, n_A)]_{dd'}^{\mu\nu} \approx -\frac{\delta dd'}{8} \bar{d}^{\mu\nu}(k, n_A) w_1^A(k). \quad (5.16)$$

A similar expression may be written down for nucleus  $B$ . Calculation of the trace over all of the multiple color and vector indices results in an overall factor of  $24 \times 32 \times T(k, q)$ . The trace  $T(k, q)$  is given below. As in Eq. (5.6) we have two types of contributions to the total cross section:

$$\sigma_g^{(0)} = \sigma_q^{(0)}(\mathcal{G}, \Pi) + \sigma_q^{(0)}(\Pi, \Pi). \quad (5.17)$$

The first term comes from the interaction of the ‘‘source’’ with the field from the ‘‘initial’’ distribution:

$$\begin{aligned} \frac{d\sigma_g^{(0)}(\mathcal{G}, \Pi)}{dp_t^2 dy} = & \frac{12\pi^2 \alpha_0}{s} \left\{ G\left(\frac{p_t e^{-y}}{\sqrt{s}}, Q_0^2\right) G'\left(\frac{p_t e^y}{\sqrt{s}}, p_t^2\right) \right. \\ & \left. \times \left[ 1 + \frac{p_t^2 e^{2y}}{s(x_A + x_B)^2} \right] + (y \rightarrow -y) \right\}. \end{aligned} \quad (5.18)$$

The second term comes from the interaction of the two sources:

$$\begin{aligned} \frac{d\sigma_g^{(0)}(\Pi, \Pi)}{dp_t^2 dy} = & \frac{24\pi\alpha_0}{sp_t^2} \int \frac{dk_t^2 dq_t^2 T(k_t, q_t)}{4S(k_t, q_t, p_t)} \\ & \times G'\left(\frac{p_t e^{-y}}{\sqrt{s}}, k_t^2\right) G'\left(\frac{p_t e^y}{\sqrt{s}}, q_t^2\right). \end{aligned} \quad (5.19)$$

The trace  $T(k, q)$  is conveniently written in the following way:

$$\begin{aligned} T(k, q) = & k_t^2 + q_t^2 \\ & + \frac{(k_t^2 + q_t^2)^2}{s(x_A + x_B)^2} \left[ \frac{q_t^2}{sx_B^2} + \frac{k_t^2}{sx_A^2} + \frac{k_t^2 q_t^2}{s^2 x_A x_B} \right] \\ & + \frac{2k_t^2 q_t^2}{s(x_A + x_B)^2} \left[ \frac{q_t^2}{sx_A^2} + \frac{k_t^2}{sx_B^2} \right]. \end{aligned} \quad (5.20)$$

The integrand of Eq. (5.19) is symmetric with respect to interchange of  $k_t$  and  $q_t$ . Hence the contribution from the interchange term ( $A \leftrightarrow B$ ) is the same, and the factor of 2 is already included in Eq. (5.19).

Equations (5.9) and (5.19) seem to have two problems. The first is an apparent infrared divergence of the total cross section due to the kinematic factor  $p_t^{-2}$ . However, one can easily see that this factor disappears when the integration variables  $k_t$  and  $q_t$  are rescaled by  $p_t$ . After such a rescaling, any remaining issues concerning low- $p_t$  behavior have to do with the sources (or structure functions), which are controlled by the data.

The second problem seems to come from the high positive powers of transverse momenta of the incoming quark and gluon fields. These can be seen in Eqs. (5.9), (5.19), and (5.20), and appear in the same form in the next perturbation order. This kind of behavior is inherent to matrix elements of processes with off-mass-shell quark and gluon initial states.

The growth of the matrix element at high transverse momenta is quite physical, and may be of interest at very small  $x$ . Indeed, wave packets with small  $x$  are smooth and extended in the longitudinal direction. If we require that large  $k_t$  and  $q_t$  add to form small  $p_t$ , then the initial geometry of the momenta is almost collinear and the incoming fields effectively overlap. We thus encounter

a type of collinear singularity which may be shielded only by an appropriate behavior of the structure functions. This is not guaranteed by the structure functions of the LLA, which evolved from the low scale via the GLAP equations. However, it is naturally provided by the BFKL equation, which leads to the asymptotic behavior (A14) also known as the random walk in transverse momentum [14]. This asymptotic behavior implies a fixed coupling constant at small  $x$ . The way the BFKL equation has been derived in Appendix A leads to a replacement of the original fixed coupling  $\alpha_s$  by the running coupling  $\alpha_s(p_i^2)$ . The BFKL equation with a running coupling constant has been conjectured in a recent paper [36], in which its solution was found numerically. Graphically, it seems to reveal a sufficient cutoff of the  $dG/dp_i^2$  at high  $p_i^2$ .

We emphasize that our approach relies on the measured DIS data. However, in the domain of very low  $x$  only very preliminary data exist at the present time.

## VI. FIRST ORDER CORRECTIONS TO THE QUARK DISTRIBUTION

In the previous section we have calculated the lowest (Born) contribution (of  $\alpha_s^0$  order) to quark and gluon production corresponding to the “excitation” of a single quark or gluon from the sea. Now we intend to show that the next order terms of our kinetic perturbation expansion describe the more usual “creation” processes. They do it in a very special way such that no infrared divergencies appear in the calculation of the total cross section. This may be the most important result of the present calculation. Furthermore, this requires no special proof: because the perturbation series for the *probabilities* was initially resumed in the new expansion, it does not generate any terms affected by the initial state collinear singularities. These are absorbed into the definition of the sources (structure functions), and thus solve the problem of divergence in an experimental way.

This is in striking contrast to all known calculations based on the factorization theorem. Such calculations always start from a *master formula*, such as

$$\begin{aligned} p^0 \frac{d\sigma(AB \rightarrow pX)}{d\mathbf{p}} &= \sum_{a,b} \sum_{c \in X} \int_0^1 dx_a \int_0^1 dx_b p^0 \frac{d\sigma(a,b \rightarrow p,c)}{d\mathbf{p}} \\ &\times F_{aA}(x_a, Q^2) F_{bB}(x_b, Q^2), \end{aligned} \quad (6.1)$$

which heavily relies on the parton model, and implicitly imparts the status of an observable to at least one additional final state particle. The  $2 \rightarrow 2$  processes have the lowest order in this approach, and the  $Q^2$  dependence of the structure functions  $F_{jJ}$  defines the so-called factorization scale, rather than reflecting its full QCD evolution. As was already mentioned in Sec. IV, the reason

structure functions are treated mistrustfully in this approach is connected with the out-of-light-cone behavior of Feynman’s propagators for the incoming partons.

Quite naturally, apart from all other amplitudes, the  $2 \rightarrow 2$  cross section includes those corresponding to the emission of a second particle  $c \in X$  from the initial state. The squared moduli of these partial amplitudes duplicate those already included in the definition of the structure functions at lower factorization scales.

The new approach does not distinguish any states absorbed into the set  $X$ . At the same time, it restores the proper status of the retarded propagation for the incoming fields. As a result, it excludes *a priori* any double counting of processes.

The first order corrections to the quark or gluon production can be divided into two major categories: the self-energy-like and the vertexlike. These names reflect only the topology of the new diagrams.

### A. Self-energy-like terms

The sequence of the  $\alpha_s$ -order diagrams in the self-energy-type term emerges from the possibility that either the quark or gluon field correlator in Eq. (5.2) represents a field in the continuum of out states,

$$\begin{aligned} p^0 \frac{dN_q}{d\mathbf{p}d^4x} &= \frac{g_0^2}{2(2\pi)^3} \int \frac{d^4k}{(2\pi)^4} \\ &\times \{ \text{Tr}[\not{p}t^a \gamma^\mu G_{01}^\#(p+k)t^b \gamma^\mu \mathbf{D}_{10,\nu\mu}^{ba}(k)] \\ &+ \text{Tr}[\not{p}t^a \gamma^\mu \mathbf{G}_{01}(p+k)t^b \gamma^\mu \mathbf{D}_{10,\nu\mu}^{\#ba}(k)] \}. \end{aligned} \quad (6.2)$$

This immediately means that the remaining exact correlators  $\mathbf{G}_{01}$  and  $\mathbf{D}_{10}$  carry information about both nucleus  $A$  and nucleus  $B$ . In other words, these fields were created during the course of the collision between the two nuclei. The only terms of the subsequent expansion of the quark and gluon correlators that survive in this case are

$$\mathbf{D}_{10} = -\mathbf{D}_{\text{ret}}^\# \Pi_{10} \mathbf{D}_{\text{adv}}^\# \quad \text{and} \quad \mathbf{G}_{01} = -\mathbf{G}_{\text{ret}}^\# \Sigma_{01} \mathbf{G}_{\text{adv}}^\#. \quad (6.3)$$

The superscript “#” indicates that we consider propagation after collision of the nuclei, and in case we need radiative corrections to this propagation we must consider them against the background of the distribution of quarks and gluons created in the collision itself.

The intensities  $\Pi$  and  $\Sigma$  of the field sources created by the two nuclei were already calculated in the previous section, but now these fields are off mass shell, and the terms with products of two \*-labeled correlators from Eqs. (5.4) should be added. These are just the lowest-order terms of the master formula (6.1) of the QCD parton model, with a fixed factorization scale  $Q_0^2$ , and correspond to processes of the type  $2 \rightarrow 2$ , where parameters of the second emitted particle are completely integrated over. Thus the complete formula will be

$$\begin{aligned} p^0 \frac{dN_q}{d\mathbf{p}d^4x} &= \frac{-g_0^2}{2(2\pi)^3} \int \frac{d^4k d^4q}{(2\pi)^4} \{ \text{Tr}[\not{p}t^a \gamma^\mu G_{01}^\#(p+k)t^b \gamma^\mu [\mathbf{D}_{\text{ret}}^\#(k) \Pi_{10}^{AB}(k) \mathbf{D}_{\text{adv}}^\#(k)]_{\nu\mu}^{ba}] \\ &+ \text{Tr}[\not{p}t^a \gamma^\mu [\mathbf{G}_{\text{ret}}^\#(k) \Sigma_{01}^{AB}(k) \mathbf{G}_{\text{adv}}^\#(k)] t^b \gamma^\mu \mathbf{D}_{10,\nu\mu}^{\#ba}(k-p)] \}, \end{aligned} \quad (6.4)$$

where the following chain of substitutions is supposed:

$$\begin{aligned} \Sigma_{01}^{AB}(p) = & ig_0^2 \int \frac{d^4 k}{(2\pi)^4} \delta(k+q-p) \{t^a \gamma^\mu [G_{01}^{B*}(k) - \mathbf{G}_{\text{ret}}(k) \Sigma_{01}^B(k) \mathbf{G}_{\text{adv}}(k)] t^b \gamma^\mu \\ & \times [D_{10}^{A*}(q) - \mathbf{D}_{\text{ret}}(q) \Pi_{10}^A(q) \mathbf{D}_{\text{adv}}(q)]_{ba, \nu\mu} + (A \leftrightarrow B)\} \end{aligned} \quad (6.5)$$

for the ‘‘collective’’ quark source, and

$$\begin{aligned} \Pi_{01}^{AB}(p) = & -ig_0^2 \int \frac{d^4 k d^4 q}{(2\pi)^4} \{V[D_{10}^{B*}(k) - \mathbf{D}_{\text{ret}}(k) \Pi_{10}^B(k) \mathbf{D}_{\text{adv}}(k)] V[D_{10}^{A*}(q) - \mathbf{D}_{\text{ret}}(q) \Pi_{10}^A(q) \mathbf{D}_{\text{adv}}(q)] \\ & + \text{Tr} t \gamma [G_{01}^{B*}(k) - \mathbf{G}_{\text{ret}}(k) \Sigma_{01}^B(k) \mathbf{G}_{\text{adv}}(k)] t \gamma [G_{10}^{A*}(q) - \mathbf{G}_{\text{ret}}(q) \Sigma_{10}^A(q) \mathbf{G}_{\text{adv}}(q)]\} \delta(k+q-p), \end{aligned} \quad (6.6)$$

for the ‘‘collective’’ gluon source. Here  $V$ 's stand for the three-gluon vertex with all arguments dropped.

Three of the six graphs of this type are given in Fig. 2. The first corresponds to the  $s$ -channel part of the Compton process. The other two are of an annihilation type. They can all be represented as squared moduli of the corresponding amplitudes. The  $t$ -channel partners of these diagrams are not generated by this perturbative expansion. If they were, they would duplicate processes already included in the definition of the sources. The three omitted graphs correspond to the interchange ( $A \leftrightarrow B$ ).

### B. First order terms from the ‘‘vertexlike’’ corrections

The general expressions for the one-particle quark and gluon distributions [Eqs. (2.10) and (2.13)] contain dressed quark-gluon and three-gluon vertices

$$\begin{aligned} \Gamma_{SQ,P}^{d,\lambda}(\xi, y; \eta) = & (-1)^{P+S+Q} \frac{\delta[\mathbf{G}^{-1}(\xi, y)]_{SQ}}{g_r \delta \mathcal{B}_\lambda^d(\eta_P)}, \\ \mathbf{V}_{bcf,RSB}^{\nu\beta\sigma}(\xi, \eta, y) = & (-1)^{R+S+P} \frac{\delta[\mathbf{D}^{-1}(\xi, \eta)]_{RS}^{bc;\nu\beta}}{g_r \delta \mathcal{B}_\sigma^f(y_B)}. \end{aligned} \quad (6.7)$$

Because of their additional matrix structure they contain some unusual elements which should be determined now. It can be done easily by using the formal solution of the matrix Schwinger-Dyson equations:

$$\begin{aligned} [\mathbf{G}^{-1}]_{AB} &= [G^{-1}]_{AB} - \Sigma_{AB}, \\ [\mathbf{D}^{-1}]_{AB} &= [D^{-1}]_{AB} - \Pi_{AB}. \end{aligned} \quad (6.8)$$

Functional derivatives of the bare field correlators give us the bare vertices, and those of self-energies give the corrections. Using the one-loop formulas for the self-energies it is straightforward to find the first order corrections to the vertices:

$$\begin{aligned} {}^{(1)}\Gamma_{RB,S}^{d,\lambda}(\xi, y; \eta) = & -ig_r^2 (-1)^{R+S} \{ \gamma^\rho t^a \mathbf{G}_{RS}(\xi, \zeta) \gamma^\lambda t^d \\ & \times \mathbf{G}_{SB}(\zeta, y) \gamma^\sigma t^b \mathbf{D}_{SR}^{ba;\sigma\rho}(y, \xi) \\ & + \gamma^\rho t^a \mathbf{G}_{RB}(\xi, y) \gamma^\sigma t^b \mathbf{D}_{BS}^{bc;\sigma\beta}(y, \zeta) \\ & \times V_{\alpha\beta\lambda}^{cgd}(\zeta) \mathbf{D}_{BS}^{bc;\alpha\rho}(\zeta, \xi) \}. \end{aligned} \quad (6.9)$$

Equation (6.9) contains an additional rule: besides the

expected contour indices, the correction  ${}^{(1)}\Gamma_{RB,S}^{d,\lambda}(\xi, y; \eta)$  to the bare vertex with the contour index  $B$  acquires an additional factor  $(-1)^{R+S}$ . This rule works in the same way for the three-gluon vertex, which is too cumbersome to be written down separately.

The sum over the contour indices naturally divides into two groups: those with  $R = S$  and those with  $R \neq S$ . We delay discussion of the first group which is responsible for those types of radiative corrections which may lead to vertex form factors. The second group, which we will discuss below, describes contributions of the higher-order real processes, like emission of a second uncontrolled jet.

The one-loop vertex-type correction to single light quark production contains four terms, two from the first term in Eq. (6.9) and two from the second one:

$$p^0 \frac{dN_q}{d\mathbf{p} d^4 x} = \frac{-ig_0^2}{2(2\pi)^3} \sum_{j=1}^4 \int \frac{d^4 k d^4 q}{(2\pi)^8} \text{Tr} [\not{p} \mathcal{I}_j(p, k, q)], \quad (6.10)$$

where

$$\begin{aligned} \mathcal{I}_1 = & t^a \gamma^\mu \mathbf{G}_{01}(k) t^d \gamma^\sigma \mathbf{G}_{10}(k+q-p) t^c \gamma^\rho \mathbf{G}_{01}(q) \\ & \times t^b \gamma^\nu \mathbf{D}_{00,\mu\rho}^{ac}(p-k) \mathbf{D}_{11,\sigma\nu}^{db}(p-q), \\ \mathcal{I}_2 = & t^a \gamma^\mu \mathbf{G}_{00}(p-k) t^d \gamma^\sigma \mathbf{G}_{01}(p-k-q) \\ & \times t^c \gamma^\rho \mathbf{G}_{11}(p-q) t^b \gamma^\nu \mathbf{D}_{01,\mu\rho}^{ac}(k) \mathbf{D}_{01,\sigma\nu}^{db}(q), \\ \mathcal{I}_3 = & t^a \gamma^\mu \mathbf{G}_{00}(p-k) t^c \gamma^\sigma \mathbf{G}_{01}(q) t^b \gamma^\nu \mathbf{D}_{01,\mu\rho}^{aa'}(k) \\ & \times \mathbf{D}_{01,\lambda\sigma}^{cc'}(k+q-p) \mathbf{D}_{11,\phi\nu}^{b'b}(p-q) \\ & \times V_{a'b'c'}^{\rho\lambda\phi}(-k, k+q-p, p-q), \\ \mathcal{I}_4 = & t^a \gamma^\mu \mathbf{G}_{01}(k) t^c \gamma^\sigma \mathbf{G}_{11}(p-q) t^b \gamma^\nu \mathbf{D}_{00,\mu\rho}^{aa'}(p-k) \\ & \times \mathbf{D}_{01,\lambda\sigma}^{cc'}(p-k-q) \mathbf{D}_{01,\phi\nu}^{b'b}(q) \\ & \times V_{a'b'c'}^{\rho\lambda\phi}(k-p, k+q-p, q). \end{aligned} \quad (6.11)$$

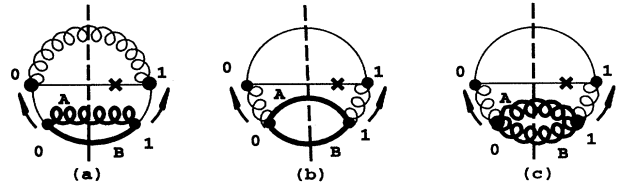


FIG. 2. Self-energy-type first order diagrams for one-quark production. Notation the same as in Fig. 1. Arrows label the retarded and advanced propagators and show the latest time.

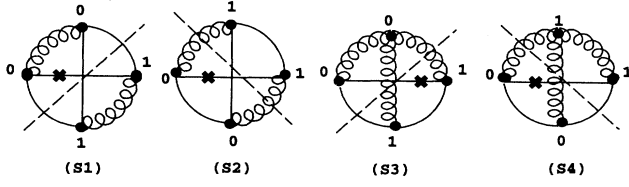


FIG. 3. Four topologies of the vertex-type diagrams for one-quark production.

These four terms are depicted in Fig. 3. There are three cut lines in each diagram, and they can be “distributed” in six different ways between the two colliding nuclei and the additional out state excited in the continuum. After that we can convert every term of this expansion into a product of two scattering amplitudes. This is done in Fig. 4 (up to a trivial interchange  $A \leftrightarrow B$ ). It is clearly seen that amongst this group of graphs there are none which would represent the squared moduli of any amplitude, but all allowed interference terms between all the processes which produce a quark and something else are included.

Recalling the previous discussion of the self-energy-type terms, we see that our perturbative expansion does not generate any diagrams which would repeat those present in the definition of the sources (via their ladder expansion). These missing patterns are not IR safe, and were regularized and renormalized in the course of their definition via the DIS cross section.

We shall now show that no further infrared problems appear. We demonstrate this using the definite subprocess of a detected quark with momentum  $p$  accompanied by an uncontrolled antiquark in the out state. They were both created in a collision of two gluons,  $g_A g_B \rightarrow q \bar{q}$ .

$$p^0 \frac{dN_q}{d\mathbf{p}d^4x} = \frac{-ig_0^2}{2(2\pi)^3} \int \frac{d^4k d^4q}{(2\pi)^8} \text{Tr}[\not{p}t^a \gamma^\mu \mathbf{G}_{00}(p-k)t^d \gamma^\sigma \mathbf{G}_{01}(p-k-q)t^c \gamma^\rho \mathbf{G}_{11}(p-q)t^b \gamma^\nu] \\ \times \left[ D_{01}^{(A)*}(k) - \mathbf{D}_{\text{ret}}^{(A)}(k) \Pi_{10}^{(A)}(k) \mathbf{D}_{\text{adv}}^{(A)}(k) \right]_{\rho\mu}^{ac} \left[ D_{10}^{(B)*}(q) - \mathbf{D}_{\text{ret}}^{(B)}(q) \Pi_{10}^{(B)}(q) \mathbf{D}_{\text{adv}}^{(B)}(q) \right]_{\sigma\nu}^{bd}, \quad (6.12)$$

where retarded and advanced functions carry a superscript indicating which nucleus was the source of field. The natural variables for subsequent calculations are quark rapidity and momentum fractions defined via

$$p^\pm = p_t e^{\pm y}, \quad k^+ = \sqrt{s} x_A, \quad q^- = \sqrt{s} x_B.$$

The most troublesome element in all following calculations is the trace over spinor and vector indices,

$$T = \text{Tr}[\not{p} \gamma^\mu (\not{p} - \not{k}) \gamma^\sigma (\not{p} - \not{k} - \not{q}) \gamma^\rho (\not{p} - \not{q}) \gamma^\nu] \\ \times d_{\rho\mu}(k, n_A) d_{\sigma\nu}(q, n_B). \quad (6.13)$$

$$\frac{d\sigma_q^{(1)}(\mathcal{G}, \mathcal{G})}{dp_t^2 dy} = -\frac{\pi\alpha_0^2}{12s^2} \int_0^1 \frac{dx_A dx_B}{x_A x_B} \left[ 1 - \frac{8p_t^2}{s x_A x_B} \right] G(x_A, Q_0^2) G(x_B, Q_0^2) \\ \times \delta \left[ x_A x_B - \frac{p_t}{\sqrt{s}} (x_A e^{-y} + x_B e^y) \right] \theta \left( x_A - \frac{p_t}{\sqrt{s}} e^y \right) \theta \left( x_B - \frac{p_t}{\sqrt{s}} e^{-y} \right). \quad (6.15)$$

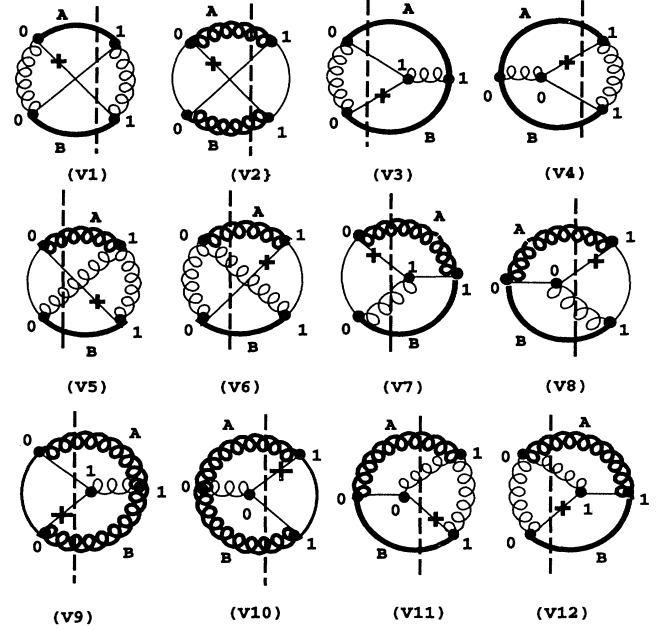


FIG. 4. Twelve vertex-type diagrams for one-quark production in first order.

### C. Infrared safety in the $\alpha_s$ order

Infrared finiteness of the self-energy-type diagrams of Fig. 2 is intuitively understandable, since the intermediate  $s$ -channel gluon or quark carries a large timelike momentum. We may expect IR problems only in the vertex-type diagrams, like (V1) of Fig. 4, where the intermediate fermion is in the  $t$  channel. The corresponding distribution of a single quark is given by the expression.

As in the lowest order, we can single out different types of terms contributing to the cross section in the first order:

$$\sigma_q^{(1)} = \sigma_q^{(1)}(\mathcal{G}, \mathcal{G}) + \sigma_q^{(1)}(\mathcal{G}, \Pi) + \sigma_q^{(1)}(\Pi, \Pi). \quad (6.14)$$

The first term corresponds to the first nonvanishing order of the master formula of the parton model, which factorizes the “hard” QCD cross section and structure functions evaluated at some (sufficiently high) scale  $Q_0^2$ . Two mass-shell  $\delta$  functions make the calculations relatively simple, and the result reads as follows:

We see that this term remains finite when  $p_t \rightarrow 0$  and is strongly suppressed, both by the second power of  $s$  in the denominator and the smallness of  $\alpha_0^2$ .

To facilitate the following analysis, let us trace how the structure emerges. We may expect an infrared divergence from the poles of the product of the two  $t$ -channel propagators in Eq. (6.12),  $G_{00}(p-k)G_{11}(p-q)$ . Since they are unshielded by finite masses or virtualities, the factor  $(p_t^2 s x_A x_B)^{-1}$  appears. One power of  $s^{-1}$  comes from the definition of cross section, and one more from the final state phase space. The combined spinor-vector trace in (6.14) gives a factor  $p_t^2 s$ . As a result, no large logarithm, which could partially compensate for the smallness of the coupling constant, appears in the total cross section. Eventually, we may expect only a weak scale dependence of the total cross section.

The “box diagram,” which is an unavoidable partner of  $\sigma_q^{(1)}(\mathcal{G}, \mathcal{G})$  in the approach based on the factorization theorem, is IR divergent, but it has no analog in our perturbation expansion. Nevertheless, we considered it useful to calculate it in Appendix B, in order to compare its structure with that emerging from the present calculations.

The mixed term  $\sigma_q^{(1)}(\mathcal{G}, \Pi)$ , and the term  $\sigma_q^{(1)}(\Pi, \Pi)$  (contributed to by two “sources”) are more complicated because one or both of the incoming fields interact with their sources and hence are off the mass shell. This means that at least one of the mass-shell  $\delta$  functions is no longer present, and traces become unwieldy. We will not present their explicit form here, as these terms are not expected to be large. Indeed, after the box diagram has been extracted, one retains only interference terms. These are usually small, unless they are affected by singular infrared behavior. A sufficient qualitative analysis of this behavior can be done without explicit calculations. It is enough to notice that the trace  $T(p, k, q)$  in the numerator of the integrand of Eq. (6.12) is, in general, a polynomial of fourth order with respect to  $p_t/\sqrt{s}$ . When the momenta of both structure functions are put on mass shell, the only powers that survive are  $p_t^2/s$  and  $p_t^4/s^2$ . This leads to an immediate cancellation of the two unshielded infrared poles of the propagators. In the integral for  $\sigma_q^{(1)}(\Pi, \Pi)$  both poles are shielded by gluon virtualities, and infrared divergence cannot appear at all. In the integral for  $\sigma_q^{(1)}(\mathcal{G}, \Pi)$  only one pole is shielded, while the second produces an unpleasant  $p_t^{-1}$  behavior. However, this does not lead to an infrared divergence of the cross section, since the same power  $p_t^{-1}$  is implicitly present in the differential  $dp_t^2$  on the LHS.

In Appendix B we consider in full the  $s$ -channel production of light quarks from the process  $gg \rightarrow q\bar{q}$ . The mathematical details behind the above qualitative analysis can be found there. Here we shall discuss only the main physical issues.

The higher powers of  $p_t$  in the trace (6.13) lead to an increase in the differential cross section at high  $p_t$  over the lowest-order result. This is in compliance with the observation that the first order terms bring more than a simple quantitative correction to the lowest order. It is precisely the emission of two back-to-back jets which

makes possible the existence of a high- $p_t$  particle in the final state.

## VII. CONCLUSION

We have considered a new approach to computing the distributions of quarks and gluons created in the first hard interaction of two heavy ions at high energies. We essentially employed an initial resummation of the perturbation series for the probabilities [5]. It allowed us to describe two different high-energy processes, viz.,  $e$ - $p$  scattering and nuclear interactions, in the same terms, as two versions of the same phenomenon—deeply inelastic scattering of composite systems.

It is shown that these calculations can be performed without reference to parton phenomenology. We have introduced the concept of a source as the main subject of QCD evolution, and have shown that the equations which describe the dynamics of the sources are independent of the type of high-energy process, and independent of the particular choice of the final interaction.

The additional benefit of the new approach is that it explicitly displays the causal structure of the QCD evolution equations; furthermore, it shows their physical meaning as the spectral analysis of the composite system, as performed by the interaction, which results in the bare quark or gluon production. The evolution equations for the sources allow for a smooth transition between the regimes described by the GLAP and BFKL equations. The by-product of this study is a new form of fusion term in the GLR-type equation, which might lead to stronger low- $x$  saturation of the sources than any terms considered previously.

One of the most important results of this study is the new type of perturbation expansion, which, unlike the factorization technique, does not lead to double counting of processes. The diagrams already included in the definition of the sources, and controlled in aggregate by the DIS data, do not appear again in higher orders of the new perturbative expansion. The diagrams which do appear are free from initial state infrared (collinear) singularities and do not require artificial cutoffs. The leading parts of these diagrams do not depend upon the initial factorization scale either. The price one pays for the efficiency of these calculations is that one requires the full  $x$  and  $Q^2$  dependence of the sources (or structure functions) extracted from the data.

We are now in a position to calculate the single-particle distributions of the quarks and gluons after the first 0.1 fm of the heavy ion collision.

## ACKNOWLEDGMENTS

I am grateful to L. McLerran, E. Levin, A. H. Mueller, E. Shuryak, J. Smith, A. Vainshtein, R. Venugopalan, and G. Welke for many stimulating discussions. This work was supported by the U.S. Department of Energy under Contract No. DE-FG02-94ER40831.

### APPENDIX A: THE FULL FORM OF THE EVOLUTION EQUATIONS

In the main body of the paper, we explicitly studied only that part of the evolution equations which eventually results in the GLAP equations. The latter are also known as the leading logarithmic approximation (LLA). Corrections to Eqs. (4.3) and (4.4) are of various origins. Unfortunately, we cannot count these corrections in the traditional way, which relies on the firm hierarchy of twists in OPE-based calculations. For the moment, by “next approximation” we shall mean some kind of structural expansion based on the complexity of the processes taken into consideration. Surprisingly, it does not lead far from the commonly used scheme.

In what follows, we study two types of corrections. First, we consider the terms missing in the analysis of the simplest (by their structure) equations, (4.3) and (4.4). In the next two subsections we study the low- $x$  region which results in the BFKL equation [13] as the limit of new evolution equations. More complicated corrections lead to an equation resembling the GLR equation [14,15], but with some significant differences.

#### 1. Trivial corrections

The simplest corrections arise from Eqs. (4.3) and (4.4), as a residue of the original spinor and tensor form after LLA terms have been extracted. To make them more visible, let us split  $\sigma_1(p)$  and  $w_1(p)$  into a leading ( $\sigma'_1$  and  $w'_1$ ) part, corresponding to the LLA, and sub-leading parts ( $\sigma''_1, w''_1, \dots$ ):

$$\begin{aligned}\sigma_1(p) &= \sigma'_1(p) + \sigma''_1(p) + \sigma'''_1(p), \\ w_1(p) &= w'_1(p) + w''_1(p) + w'''_1(p).\end{aligned}\quad (\text{A1})$$

The mathematical steps follow those of the perturbation calculations described in Sec. III. Now it is only a lengthy exercise to obtain the resulting equations. Spinor components of the quark source may be expanded as follows:

$$\begin{aligned}\sigma'_1(p) &= \int d^4k \Delta_{kp} \frac{-p^2 k^+}{p^+} \left[ P_{qq} \left( \frac{p^+}{k^+} \right) \frac{k^+ \sigma_1(k)}{\mathcal{S}_1^R(k) \mathcal{S}_1^A(k)} \right. \\ &\quad \left. + P_{qg} \left( \frac{p^+}{k^+} \right) \frac{k^+ w_1(k)}{\mathcal{W}_1^R(k) \mathcal{W}_1^A(k)} \right],\end{aligned}\quad (\text{A2})$$

$$\begin{aligned}\sigma''_1(p) &= \int d^4k \Delta_{kp} k^2 \left[ -P_{qq} \left( \frac{p^+}{k^+} \right) \frac{k^+ \sigma_1(k)}{\mathcal{S}_1^R(k) \mathcal{S}_1^A(k)} \right. \\ &\quad \left. + P_{qg} \left( \frac{p^+}{k^+} \right) \frac{k^+ w_1(k)}{\mathcal{W}_1^R(k) \mathcal{W}_1^A(k)} \right],\end{aligned}\quad (\text{A3})$$

$$\begin{aligned}\sigma'''_1(p) &= \int d^4k \Delta_{kp} p^+ \left[ C_F \frac{\sigma_2(k)}{\mathcal{S}_2^R(k) \mathcal{S}_2^A(k)} \right. \\ &\quad \left. + \left( 1 - \frac{p^+}{k^+} \right) \frac{k^2 w_2(k)}{\mathcal{W}_2^R(k) \mathcal{W}_2^A(k)} \right],\end{aligned}\quad (\text{A4})$$

$$\begin{aligned}\sigma_2(p) &= \int d^4k \Delta_{kp} \frac{k^+}{p^+} \left[ C_F \frac{k^+ \sigma_1(k)}{\mathcal{S}_1^R(k) \mathcal{S}_1^A(k)} \right. \\ &\quad \left. + \left( 1 - \frac{p^+}{k^+} \right) \frac{k^+ w_1(k)}{\mathcal{W}_1^R(k) \mathcal{W}_1^A(k)} \right],\end{aligned}\quad (\text{A5})$$

where we have denoted

$$\begin{aligned}\Delta_{kp} &= \frac{2g_r^2}{(2\pi)^3 k^+} \delta^+[(k-p)^2] \\ &= \frac{2g_r^2 \theta(k^0 - p^0)}{(2\pi)^3 k^+} \delta[(p^+ - k^+)(p^- - k^-) \\ &\quad - (\mathbf{p}_t - \mathbf{k}_t)^2].\end{aligned}$$

The meaning of this decomposition becomes clear if we multiply it by the kinematic factor  $p^+$  and sandwich it between retarded and advanced propagators [see Eq. (4.13)]. The joint left-hand side of Eqs. (A2)–(A4) becomes the derivative with respect to  $Q^2$  of the quark structure function of DIS. The RHS of Eq. (A2) then leads to the GLAP part of the evolution. The factor  $p^2$  in it is responsible for the logarithmic behavior. Now it is easy to see that the RHS of (A3) will result in a term with  $1/Q^2$  behavior. It simulates the next twist contribution, even though the second twist is not included explicitly in the density matrix as an effect of next order correlations.

The RHS of (A4) represents a secondary influence of the longitudinal components of the spinor and gluon sources. These components are defined by (A5) and (A8), and are of next order by a formal count of the  $\alpha_s$  powers.  $\sigma_2$  directly contributes to the longitudinal structure function given by Eq. (4.15). It also appears in the Born term of the quark excitation process, but we leave it aside for now since it is poorly controlled by the data.

All of the above comments apply equally to the components of the gluon source, which can be decomposed following the same principle:

$$\begin{aligned}w'_1(p) &= \int d^4k \Delta_{kp} \frac{-p^2 k^+}{p^+} q \left[ P_{gq} \left( \frac{p^+}{k^+} \right) \frac{k^+ \sigma_1(k)}{\mathcal{S}_1^R(k) \mathcal{S}_1^A(k)} \right. \\ &\quad \left. + P_{gg} \left( \frac{p^+}{k^+} \right) \frac{k^+ w_1(k)}{\mathcal{W}_1^R(k) \mathcal{W}_1^A(k)} \right],\end{aligned}\quad (\text{A6})$$

$$\begin{aligned}w''_1(p) &= \int d^4k \Delta_{kp} k^2 \left[ P_{gq} \left( \frac{p^+}{k^+} \right) \frac{k^+ \sigma_1(k)}{\mathcal{S}_1^R(k) \mathcal{S}_1^A(k)} \right. \\ &\quad \left. + P_{gg} \left( \frac{p^+}{k^+} \right) \frac{k^+ w_1(k)}{\mathcal{W}_1^R(k) \mathcal{W}_1^A(k)} \right],\end{aligned}\quad (\text{A7})$$

$$\begin{aligned}w'''_1(p) &= \int d^4k \Delta_{kp} k^+ \left[ C_F \left( 1 - \frac{p^+}{k^+} \right) \frac{\sigma_2(k)}{\mathcal{S}_2^R(k) \mathcal{S}_2^A(k)} \right. \\ &\quad \left. - 2N_c \left( \frac{p^+}{k^+} - \frac{1}{2} \right)^2 \frac{k^2 w_2(k)}{\mathcal{W}_2^R(k) \mathcal{W}_2^A(k)} \right],\end{aligned}\quad (\text{A8})$$

$$\frac{w_2(p)}{p^2} = \int d^4k \Delta_{kp} \frac{k^+}{p^+} \left[ -8C_{Fnf} \left(1 - \frac{p^+}{k^+}\right) \frac{k^+ \sigma_1(k)}{S_1^R(k) S_1^A(k)} + 4N_c \frac{k^+}{p^+} \left(1 - \frac{p^+}{2k^+}\right)^2 \frac{k^+ w_1(k)}{\mathcal{W}_1^R(k) \mathcal{W}_1^A(k)} \right]. \quad (\text{A9})$$

A preliminary examination of the additional terms in the evolution equations reveals that they have the same singular infrared behavior as GLAP equations, and should be regularized and renormalized. The way to do this is not yet clear, since conservation of momentum seemingly fails to control all necessary subtractions. A complete study of these equations is a separate subject. In this paper, we have considered the explicit form of the DIS structure functions as granted.

## 2. The BFKL equation

As has been shown in Sec. IV, the new evolution equations for the sources, even in their reduced form (4.3) and (4.4), are practically the equations for the derivatives of the structure functions, rather than for the DIS structure functions themselves. The former were first introduced by Lipatov as the “unintegrated structure functions,” and they relate to the latter in the following way:

$$f(x, p_t^2) = p_t^2 \frac{d x G(x, p_t^2)}{d p_t^2}. \quad (\text{A10})$$

Thus, up to an insignificant normalization factor, we may write

$$\delta(p^-) f(x, p_t^2) = \frac{i x^2 p_t^2 w_1^{01}(p)}{\mathcal{W}_1^R(p) \mathcal{W}_1^A(p)}. \quad (\text{A11})$$

In the limit of low  $x$ , the function  $f(x, p_t^2)$  was proven to obey the so-called BFKL equation,

$$-x \frac{\partial f(x, p_t^2)}{\partial x} = \frac{3\alpha_s}{\pi} p_t^2 \int_0^\infty \frac{d k_t^2}{k_t^2} \left[ \frac{f(x, k_t^2) - f(x, p_t^2)}{|p_t^2 - k_t^2|} + \frac{f(x, p_t^2)}{\sqrt{4k_t^4 - p_t^4}} \right]. \quad (\text{A12})$$

This equation was originally obtained by considering the amplitude of the process  $2 \rightarrow 2 + n$  and summing the leading  $\log(1/x)$  terms [13].

Evolution equations like (4.4) were derived immediately as integral equations. At high  $Q^2$  and not too low  $x$ , they allow for simplifications which lead to the GLAP equations. This means that the necessary resummation of the leading  $\ln Q^2$  was done from the very beginning. Next, our intention is to determine what simplifications should be done to obtain the BFKL equation. These simplifications are effectively equivalent to a reduction in the number of diagrams already accounted for in the integral equation.

In the notation of Eq. (A10), our Eq. (4.10) for the transverse gluon source reads

$$\begin{aligned} \delta(p^-) f(x, p_t^2) &= \frac{\alpha_s(p_t^2)}{2\pi^2} x p_t^2 \int_x^1 \frac{dy}{y} \int \frac{d^2 \mathbf{k}_t}{k_t^2} \\ &\times \delta[(p^+ - k^+) p^- - (\mathbf{p}_t - \mathbf{k}_t)^2] \\ &\times \left[ \frac{-p^2}{\mathcal{W}_1^R(p) \mathcal{W}_1^A(p)} \right] P_{gg} \left( \frac{x}{y} \right) f(y, k_t^2). \end{aligned} \quad (\text{A13})$$

We have retained all terms that contribute to the LLA. We notice that at real momenta the denominator  $\mathcal{W}_1^R(p) \mathcal{W}_1^A(p)$  is strictly positive both before and after any integration, without additional weight. Thus the full integral is not singular. The next steps are as follows.

*Step 1.* For  $x \ll 1$ , approximate the splitting kernel as  $P_{gg}(x/y) \sim (y/x)$ .

*Step 2.* Integrate both sides of the equation over  $p^-$ , considering the retarded and advanced propagators in the integrand on the RHS as bare. In this way the singular infrared behavior of the integrand is unshielded. Integrate over the azimuthal angle.

*Step 3.* Expand the propagators on the LHS up to the first order in radiative corrections. Retain only the vacuum correlator and move it to the RHS in order to shield the singularity that resulted from the approximation.

*Step 4.* Differentiate both sides of the equation with respect to  $x$ .

This procedure will result in the BFKL equation (A12), up to the insignificant last term in the integrand and significant replacement of the fixed coupling by the running one. The latter is prescribed for us by the renormalization scheme described in Sec. IV B. Unlike the OPE-based approach, this scheme has no limitations at small  $x$ .

The asymptotic behavior of the solution with the fixed coupling constant is well known. Its exponential part,

$$f(x, p_t^2) \sim \exp \left( \frac{-\ln^2(p_t^2/\bar{p}_t^2)}{2\lambda' \ln(x_0/x)} \right), \quad (\text{A14})$$

provides a decrease of  $f(x, p_t^2)$  at high  $p_t^2$  that is faster than any negative power of  $p_t^2$ .

The BFKL equation modified by the standard running coupling was recently conjectured in Ref. [36], and studied numerically. Visually, the plots reveal a sufficiently steep behavior at high  $k_t^2$ , but further analytic analysis is required to draw a firm conclusion. A less trivial modification of the BFKL equation was recently suggested in Ref. [37].

We postpone any discussion of the accuracy of the above approximation, and satisfy ourselves with the most important fact that the evolution equations contain both GLAP and BFKL regimes of evolution as the limits. Thus we may hope to describe a smooth transition between them. From a pragmatic point of view, the above asymptotic behavior guarantees the convergence of the integrals that appear in a calculation of the cross sections of quark and gluon production (see Secs. V and VI).

## 3. Gluon shadowing

More complex corrections to the GLAP evolution correspond to the replacement of the #-labeled correlators

in Eqs. (4.3) and (4.4) by correlators with sources, viz., the second terms in Eqs. (4.1) and (4.2). This means that, instead of the final state correlators describing the emission, we include the initial state correlators. This replacement accounts for possible fusion of the partons. Fusion is expected to be most important for gluons at low  $x$ . So only the purely gluonic component will be considered here.

Terms responsible for fusion of two gluon fields have the form

$$\begin{aligned} \Delta_{\text{fus}}\Pi_{01}^{ab,\mu\nu}(p) &= ig_r^2 \int \frac{d^4k d^4q}{(2\pi)^4} \delta(k+q-p) V_{acf}^{\mu\rho\sigma}(k+q, -q, -k) \\ &\times [D_{\text{ret}}(k)\Pi_{10}(k)D_{\text{adv}}(k)]_{ff'}^{\sigma\beta} V_{bc'f'}^{\nu\lambda\beta}(-k-q, q, kk) [D_{\text{ret}}(q)\Pi_{10}(q)D_{\text{adv}}(q)]_{cc'}^{\rho\lambda}. \end{aligned} \quad (\text{A15})$$

This equation is identical to Eq. (5.15) describing gluon fusion in a nuclear collision, except that here both gluons are taken from the same nucleus. We shall use the standard approximation, i.e., bare tree propagators and bare vertices. The longitudinal gluon function  $w_2$  will be neglected also. Routine calculations similar to those performed in Sec. V then yield

$$\begin{aligned} \Delta_{\text{fus}}G'(x, p_t^2) &= -\frac{3\pi\alpha_0}{2p_t^4} \frac{(2\pi)^3}{\pi R^2} x^2 \int_0^x \frac{dx_1}{x_1} \int_0^x \frac{dx_2}{x_2} \delta(x_1+x_2-x) \int \frac{dk_t^2 dq_t^2}{4S(k_t, q_t, p_t)} \\ &\times \left[ \frac{x^2}{x_1x_2} - \frac{x_1x_2}{x^2} \right]^2 \left[ \frac{k_t^2}{x_1} + \frac{q_t^2}{x_2} - \frac{p_t^2}{x} \right] G'(x_1, k_t^2) G'(x_2, q_t^2), \end{aligned} \quad (\text{A16})$$

where  $G'(x, p_t^2) = dG(x, p_t^2)/dp_t^2$  and  $S(k_t, q_t, p_t)$  is the area of a triangle with the sides  $k_t$ ,  $q_t$ , and  $p_t$ . The initial normalization factor  $(V_{\text{lab}}P^+)^{-1}$ , which was convenient for calculation of cross sections, has been replaced in Eq. (A16) by  $(\pi R^2)^{-1}$ , which corresponds to a normalization per unit transverse area of a nucleus with radius  $R$ .

Equation (A16), by its structure, is very similar to the well known Gribov-Levin-Ryskin (GLR) equation [14], and one derived later by Mueller and Qui [15]. It clearly reveals the same tendency to saturate the rate of the field source QCD evolution at low  $x$ . However, it seems to have several differences. The most significant is that the power of  $\alpha_s$  in Eq. (A16) is less than in Refs. [14] and [15]. The formal reason is the simpler form of the vertex

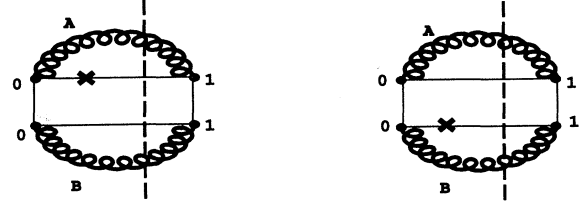


FIG. 5. Two infrared-divergent “box” diagrams which are not generated by our perturbation theory.

of the “three-ladder interaction” that is prescribed for us by the general structure of the evolution equations (4.3) and (4.4). The other differences are of dynamic origin and will be discussed elsewhere.

## APPENDIX B: SOME ESTIMATES OF THE FIRST ORDER TERMS

### 1. The “box” diagram

Two box-type diagrams appear in the calculation of the quark production cross section, if we use the master formula (6.1). They are depicted in Fig. 5, and the corresponding analytic formula is

$$\begin{aligned} 2p^0 \frac{dN_q^{\text{box}}}{dp^4 dx} &= \frac{-ig_0^2}{(2\pi)^3} \int \frac{d^4k d^4q}{(2\pi)^8} [\text{Tr} \not{p} \not{t}^a \gamma^\mu \mathbf{G}_{\text{ret}}(p-q) \not{t}^d \gamma^\sigma \mathbf{G}_{01}^\#(p-k-q) \not{t}^c \gamma^\rho \\ &\times \mathbf{G}_{\text{adv}}(p-q) \not{t}^b \gamma^\nu \mathbf{D}_{01,\sigma\rho}^{(A)dc}(k) \mathbf{D}_{01,\nu\mu}^{(B)ab}(q) + (A \leftrightarrow B)]. \end{aligned} \quad (\text{B1})$$

Routine calculations result in the following expression for the differential cross section:

$$\begin{aligned} \frac{d\sigma_q^{(\text{box})}(\mathcal{G}, \mathcal{G})}{dp_t^2 dy} &= -\frac{2\pi\alpha_0^2}{3sp_t^2} \int_0^1 \frac{dx_A dx_B}{x_A x_B} \theta\left(x_A - \frac{p_t}{\sqrt{s}} e^y\right) \theta\left(x_B - \frac{p_t}{\sqrt{s}} e^{-y}\right) \\ &\times \left[ 1 - \frac{p_t^2(3 - x_A x_B)}{s x_A x_B} - \frac{4p_t^4}{(s x_A x_B)^2} \right] G(x_A, Q_0^2) G(x_B, Q_0^2) \delta\left[x_A x_B - \frac{p_t}{\sqrt{s}} (x_A e^{-y} + x_B e^y)\right]. \end{aligned} \quad (\text{B2})$$

The factor  $p_t^{-2}$  appears in the same way as in Eq. (5.9) for the Born term. However, previously it could be effectively absorbed into the structure functions, which is not the case now. Indeed, Eq. (B2) has no additional integration over momenta which could be rescaled by  $p_t$ . We expect at least a logarithmic divergence of the total cross section as a result. This divergence may be strengthened by the low- $x$  behavior of the structure functions because of the  $p_t$  dependence of the low limits of integration over  $x_A$  and  $x_B$  in Eq. (B2).

## 2. Inclusive production of quarks in $s$ channel

The analytic expression for the diagram (S2) of Fig. 3, corresponding to the subprocess  $gg \rightarrow q\bar{q}$ , is

$$2p^0 \frac{dN_q}{d\mathbf{p}d^4x} = \frac{-ig_0^2}{(2\pi)^3} \int \frac{d^4k d^4q}{(2\pi)^8} [\text{Tr} p_t^a \gamma^\mu \mathbf{G}_{01}^\#(p-k-q) t^b \gamma^\nu \mathbf{D}_{\text{ret},\mu\lambda}^{(\#)aa'}(k+q) \mathbf{D}_{\text{adv},\gamma\rho}^{(\#)bb'}(k+q) \\ \times \{V_{acd}^{\lambda\rho\sigma}(-k-q, k, q) \mathbf{D}_{01,\rho\alpha}^{(A)cc'}(k) V_{bc'd'}^{\gamma\alpha\beta}(k+q, -k, -q) \mathbf{D}_{01,\sigma\beta}^{(B)dd'}(q) + (A \leftrightarrow B)\}]. \quad (\text{B3})$$

The most difficult problem here is to calculate the trace over spinor and vector indices. The complete expression is very unwieldy, and we will therefore satisfy ourselves with

$$\text{Trace} = 12 \times 16p_t^2 s x_A x_B [1 + O(p_t/\sqrt{s})],$$

where the factor 12 comes from the color algebra. As previously, we have three contributions to this process,

$$\sigma_q^{(2)} = \sigma_q^{(2)}(\mathcal{G}, \mathcal{G}) + \sigma_q^{(2)}(\mathcal{G}, \Pi) + \sigma_q^{(2)}(\Pi, \Pi). \quad (\text{B4})$$

The first term corresponds to the factorization of the parton's structure functions and the "hard" cross section at a given scale,

$$\frac{d\sigma_q^{(2)}(\mathcal{G}, \mathcal{G})}{dp_t^2 dy} = \frac{3\alpha_0^2 p_t^2}{2s^3} \int_0^1 \frac{dx_A dx_B}{x_A^2 x_B^2} \theta\left(x_A - \frac{p_t}{\sqrt{s}} e^y\right) \\ \times \theta\left(x_B - \frac{p_t}{\sqrt{s}} e^{-y}\right) G(x_A, Q_0^2) G(x_B, Q_0^2) \\ \times \delta\left[x_A x_B - \frac{p_t}{\sqrt{s}} (x_A e^{-y} + x_B e^y)\right]. \quad (\text{B5})$$

This term, explicitly dependent on the factorization scale, is kinematically suppressed by three powers of  $s^{-1}$ . Two of these come from the kinematics of intermediate gluons, and the third from the phase volume which is confined to a line in the  $(x_A, x_B)$  plane.

The second term in Eq. (B4) describes the interaction of a parton with the source,

$$\frac{d\sigma_q^{(2)}(\mathcal{G}, \Pi)}{dp_t^2 dy} = \frac{3\alpha_0^2 p_t^2}{16\pi^2} \int_0^1 dx_A \int_0^1 dx_B \theta\left(x_A - \frac{p_t}{\sqrt{s}} e^y\right) \theta\left(x_B - \frac{p_t}{\sqrt{s}} e^{-y}\right) \\ \times \int_{|p_t-\xi|}^{p_t+\xi} \frac{k_t dk_t}{4S(k_t, p_t, \xi)} \left[ \frac{G(x_B, Q_0^2) G'(x_A, k_t^2)}{(sx_A^2 x_B^2 - k_t^2)^2} + (A \leftrightarrow B) \right], \quad (\text{B6})$$

where we have introduced the notation

$$\xi^2 = (k^+ - p^+)(k^- - p^-) = s \left(x_A - \frac{p_t}{\sqrt{s}} e^y\right) \left(x_B - \frac{p_t}{\sqrt{s}} e^{-y}\right).$$

This second term still keeps its dependence on the factorization scale. Because of finite virtuality of one of the incoming fields, the phase volume of the process is larger and consequently one of the powers  $s^{-1}$  disappears.

The last term in Eq. (B4) accounts for the interaction of two sources,

$$\frac{d\sigma_q^{(2)}(\Pi, \Pi)}{dp_t^2 dy} = \frac{3\alpha_0^2 p_t^2}{32\pi^2} \int_0^1 dx_A \int_0^1 dx_B \theta\left(x_A - \frac{p_t}{\sqrt{s}} e^y\right) \theta\left(x_B - \frac{p_t}{\sqrt{s}} e^{-y}\right) \\ \times \int_{|p_t-\xi|}^{p_t+\xi} \frac{l_t dl_t}{4S(l_t, p_t, \xi)} \int d^2\mathbf{f} \frac{G'[x_A, (\mathbf{l}_t + \mathbf{f}_t)^2/4] G'[x_B, (\mathbf{l}_t - \mathbf{f}_t)^2/4]}{(sx_A^2 x_B^2 - l_t^2)^2}. \quad (\text{B7})$$

Here, both incoming fields are virtual, and the  $s$ -channel propagators are smoothed by the total transverse momentum of the initial fields. The internal integral over  $d^2\mathbf{f}$  represents the two-dimensional Fourier transform of the product of the densities (in coordinate space) of two sources. Hence this term is proportional to the degree of geometrical overlap between the colliding nuclei. It does not depend on a factorization scale, and is expected to

be the dominant term.

All three terms appear free of any problems at low  $p_t$ , but a reliable knowledge of the low- $x$  behavior of the sources may be important for quantitative computations. The presence of a factor  $p_t^2$ , which is purely kinematic in its origin, guarantees that at high  $p_t$  the first order differential cross section will be larger than the Born cross section in this region.

- [1] J.-P. Blaizot and A.H. Mueller, Nucl. Phys. **B289**, 847 (1987).
- [2] X.N. Wang and M. Gyulassy, in BNL RHIC Workshop, 1990, p. 79.
- [3] K. Geiger and B. Muller, Nucl. Phys. **B369**, 600 (1992).
- [4] L. McLerran and R. Venugopalan, Phys. Rev. D **49**, 2233 (1994); **49**, 3352 (1994).
- [5] A. Makhlin, Phys. Rev. C **51**, 3454 (1995).
- [6] L.V. Keldysh, Sov. Phys. JETP **20**, 1018 (1964); E.M. Lifshits and L.P. Pitaevskii, *Physical Kinetics* (Pergamon Press, Oxford, 1981).
- [7] J.C. Collins and J. Qui, Phys. Rev. D **39**, 1398 (1989).
- [8] L. Durand and W. Puttika, Phys. Rev. D **36**, 2840 (1987).
- [9] K. Geiger and B. Muller, Phys. Rev. D **50**, 337 (1994).
- [10] G. Altarelli and G. Parisi, Nucl. Phys. **B126**, 298 (1977).
- [11] L.N. Lipatov, Sov. J. Nucl. Phys. **20**, 94 (1975).
- [12] V.N. Gribov and L.N. Lipatov, Sov. J. Nucl. Phys. **15**, 438 (1975); **15**, 675 (1975); Yu.L. Dokshitzer, Sov. Phys. JETP **46**, 641 (1977).
- [13] E.A. Kuraev, L.N. Lipatov, and V.S. Fadin, Sov. Phys. JETP **45**, 199 (1977); Ya.Ya. Balitskij and L.N. Lipatov, Sov. J. Nucl. Phys. **28**, 822 (1978).
- [14] L.V. Gribov, E.M. Levin, and M.G. Ryskin, Phys. Rep. **100**, 1 (1983).
- [15] A.H. Mueller and J. Qui, Nucl. Phys. **B268**, 427 (1986).
- [16] E.V. Shuryak, Rev. Mod. Phys. **65**, 1 (1993).
- [17] S. Brodsky and H.C. Pauli, Report No. SLAC-PUB-5558, 1991.
- [18] P.A.M. Dirac, Rev. Mod. Phys. **21**, 392 (1949).
- [19] A. Makhlin, Stony Brook Report No. SUNY-NTG-93-12, 1993 (unpublished).
- [20] M. Gluck, E. Reya, and A. Vogt, Z. Phys. C **48**, 471 (1990); **53**, 471 (1992).
- [21] J.G. Morfin and W.K. Tung, Z. Phys. C **52**, 13 (1991).
- [22] A.D. Martin, R.G. Roberts, and W.J. Stirling, Phys. Rev. D **50**, 6734 (1994).
- [23] Yu.L. Dokshitzer, D.I. Dyakonov, and S.I. Troyan, Phys. Rep. **58**, 269 (1980).
- [24] N.N. Bogolyubov and D.V. Shirkov, *Introduction to the Theory of Quantized Fields* (Interscience, New York, 1959).
- [25] V. Barone *et al.*, Phys. Lett. B **304**, 176 (1993).
- [26] A.J. Askew *et al.*, Phys. Rev. D **47**, 3775 (1993); J. Blumlein, Report No. hep-ph-9408077, 1994.
- [27] ZEUS Collaboration, Report No. DESY 94-143, 1994.
- [28] H1 Collaboration, Report No. DESY 95-006, 1995.
- [29] M. Gluck, E. Reya, and M. Strautmann, Nucl. Phys. **B422**, 37 (1994).
- [30] M. Gluck, E. Hoffmann, and E. Reya, Z. Phys. C **13**, 471 (1982).
- [31] M.A.G. Aivazis, J.C. Collins, F.I. Olness, and W.-K. Tung, Phys. Rev. D **50**, 3102 (1994).
- [32] E. Laenen, S. Riemersma, J. Smith, and W.L. van Neerven, Nucl. Phys. **B392**, 162 (1993); **B392**, 229 (1993).
- [33] I. Sarcevic and P. Valerio, Phys. Lett. B **338**, 426 (1994).
- [34] S. Liuti and R. Vogt, Report No. LBL-35821 (hep-ph-9407272), 1994.
- [35] J. Collins, D. Soper, and G. Sterman, Nucl. Phys. **B263**, 37 (1986).
- [36] A.J. Askew, J. Kwiecinski, A.D. Martin, and P.J. Sutton, Phys. Rev. D **49**, 4402 (1994).
- [37] E. Levin, Report No. TAUP 2221-94 (hep-ph-9412345), 1994.